

The *curved* Mimetic Finite Difference method: allowing grids with curved faces

Silvano Pitassi^{a,*}, Riccardo Ghiloni^b, Igor Petretti^a, Francesco Trevisan^a,
Ruben Specogna^a

^a*University of Udine, Polytechnic Department of Engineering and Architecture, EMCLab,
via delle scienze 206, 33100 Udine, Italy*

^b*University of Trento, Mathematics Department, via Sommarive 14, 38123 Povo-Trento,
Italy*

Abstract

We present a new mimetic finite difference method for diffusion problems that converges on grids with *curved* (i.e., non-planar) faces. Crucially, it gives a symmetric discrete problem that uses only one discrete unknown per curved face. The principle at the core of our construction is to abandon the standard definition of local consistency of mimetic finite difference methods. Instead, we exploit the novel and global concept of P_0 -consistency. Numerical examples confirm the consistency and the optimal convergence rate of the proposed mimetic method for cubic grids with randomly perturbed nodes as well as grids with curved boundaries.

Keywords: mimetic finite difference method, generalized polyhedral meshes, curved faces, dual grid

1. Introduction

The *Mimetic Finite Difference* (MFD) method [1] is a sound numerical technique that has been applied to solve many classes of physical problems. One of its main advantages is the support of arbitrary *polyhedral grids*, i.e., meshes

*Corresponding author: Tel.: +039-0432-558037;

Email addresses: `pitassi.silvano@spes.uniud.it` (Silvano Pitassi), `riccardo.ghiloni@unitn.it` (Riccardo Ghiloni), `petretti.igor@spes.uniud.it` (Igor Petretti), `francesco.trevisan@uniud.it` (Francesco Trevisan), `ruben.specogna@uniud.it` (Ruben Specogna)

composed of general polyhedral elements with planar faces, and possibly featuring non-matching interfaces. Polyhedral grids offer several distinctive advantages: (i) their use can simplify the modeling of sharp geometric features of domains; (ii) they support non-conforming mesh refinement, which does not require to trade mesh quality for accuracy; (iii) they can be used to reduce the computational cost by mesh coarsening, where multiple elements from a (fixed) background mesh are coalesced into a single one.

However, many applications require grids whose elements have *curved* (i.e., non-planar) faces. For example, in the modeling of complex reservoir geometries in real-world geological applications or of geometries like cylinders and spheres which are of common use in electromagnetics. We emphasize that even if the computational domain is a polyhedron, curved faces may appear in the interior of the domain just because a hexahedral mesh has been obtained with an unstructured meshing algorithm.

Unfortunately, the standard MFD method does not converge on grids with curved faces [2]. In order to deal with such convergence problems, the different numerical methods proposed in literature implement two basic strategies, which, however, exhibit important limitations and downsides.

The first approach is to approximate curved faces with triangles (or more generally with polygons) to obtain a polyhedral grid where all the elements have planar faces so that we can apply the standard MFD method [2, 3]. With this approach we obtain a symmetric discrete problem but the price to pay is the additional number of discrete face unknowns, which will be proportional to the number of triangles partitioning every curved face.

The second approach proceeds in two steps: (i) a constant vector field is obtained by interpolating discrete face unknowns on every element by using standard least squares methods; (ii) mimetic inner products are constructed on every element by projecting these constant vector fields onto edges of a *dual* (or *secondary*) grid \tilde{K} [4]. A dual grid \tilde{K} is constructed by duality starting from a given discretization grid K , hence, called a *primal* grid. Here, duality is expressed as a bijective correspondence between geometric elements of the

pair of grids (K, \tilde{K}) such that to each d -dimensional geometric element in K corresponds a unique dual $(3-d)$ -dimensional geometric element in \tilde{K} . However, using this dual grid approach on curved meshes the resulting discrete problem is non-symmetric which significantly reduces the number of available efficient solution methods. Basically, the discretization methods in [5, 6] reduce to the above approach although a dual grid is not explicitly introduced.

The aim of this paper is to introduce the *curved* MFD method, an extension of the MFD method that converges on grids with curved faces. Crucially, it gives a discrete problem that is both symmetric and uses only one discrete face unknown for each curved face. Our work thus answers to an open question raised in [7, 2] on “whether the use of additional degrees of freedom is the only way to preserve symmetry in the discrete problem”. To the best of our knowledge, the numerical method presented in [7, 8] is the only low-order mimetic numerical method that converges on grids with curved faces. In particular, it results in a symmetric discrete problem which uses three discrete unknowns for each curved face (more precisely, *strongly* curved faces¹). More recently, high-order numerical methods have been developed for the treatment of 3-dimensional grids with curved faces in the context of Hybrid High Order methods [9], [10] and Virtual Element Method [11], but we note that their lowest order versions employ more than one discrete unknown per curved face and thus are not equivalent to the curved MFD method proposed in this paper. Finally, the mimetic method developed in [4] uses only one discrete unknown per curved face but is restricted to grids obtained by barycentric subdivision of tetrahedral grids, which are made of barycentric dual cells with non-planar faces.

The core idea of our method is to abandon the definition of *consistency* used in the standard MFD method. Consistency is a local property of *mimetic inner products* and *reconstruction operators* that encodes an exactness property for

¹[7] distinguishes between *moderately* and *strongly* curved faces; the distinction between the two types of curved faces is based, as the names suggest, on a measure of the curvature of faces and is used as a definition for the theoretical analysis of convergence.

constant vector fields [1]. In particular, the consistency of the standard MFD method is equivalent to the consistency enforced on the *barycentric dual grid*. In fact, as demonstrated in [12], and also as we will show in Section 4.3, reconstruction operators of the standard MFD method are equivalent to reconstruction operators of the Discrete Geometric Approach (DGA) [13]. The latter, are defined by geometric elements of the barycentric dual grid and satisfy two key properties [12]:

(P1) They provide a left inverse for local projection operators restricted to the vector subspace of constant vector fields, which is the *accuracy* or *unisolvence* property for constant vector fields [14].

(P2) Their geometric entries form closed paths supported on different elements.

The key observation is that the property **(P1)** is not valid for grids with curved faces: this is the theoretical reason for the inadequacy of the consistency of the standard MFD method on grids with curved faces.

Instead of focusing on local consistency, in our curved MFD method we employ the novel concept of P_0 -consistency introduced in [12]. In contrast with consistency of the standard MFD method, P_0 -consistency is a global property as meaning that involves reconstruction operators defined on more than one grid element. The idea underlying its definition is to abstract the properties **(P1)** and **(P2)** of the barycentric dual grid and reverse our line of reasoning: any grid whose geometric elements satisfy properties **(P1)** and **(P2)** leads to consistent reconstruction operators, precisely, P_0 -consistent reconstruction operators. We will present their formal definition in Section 3. As a side note, we would like to point that special cases of P_0 -consistent reconstruction operators have already been successfully employed in the mimetic scheme in [4].

In Section 4, we provide a geometric characterization of P_0 -consistent reconstruction operators as the affine solution space of a linear system of equations. Then, following [8], we focus on the practically important class of cubic grids with randomly perturbed nodes (according to a suitable probability distribution), and in Theorem 7, we formally demonstrate that with probability 1 there

exists at least one solution of the above mentioned linear system of equations, or equivalently, there exist P_0 -consistent reconstruction operators. Once P_0 -consistent reconstruction operators are available, local and global mass matrices are constructed just like the standard MFD method. Therefore, all the solid foundation of the standard MFD can be readily applied to our novel curved MFD method.

In Section 5 we test the curved MFD method on grids with highly curved faces and also curved boundaries, and for all the considered examples, consistency and the optimal convergence rate are achieved.

We note that the ability of expressing the standard MFD method in a geometric language is very important for improving its basic building blocks. Thus, we emphasize the importance of seeing the geometry hidden behind the standard MFD method. We believe that this geometric viewpoint might also open new perspectives on the general treatment of curved faces for high-order extensions of the MFD method like the Virtual Element Method, which is still an open problem [15]. We summarize these observations in Section 6.

2. Curved grids and geometric entities

Let Ω be a bounded domain of \mathbb{R}^3 . Here, by the term domain, we mean the closure of a connected open subset of \mathbb{R}^3 . In particular, Ω contains its boundary $\partial\Omega$. A k -cell is a k -dimensional manifold in \mathbb{R}^3 that is homeomorphic to the closed k -dimensional ball. We equip each k -cell in K with an inner orientation [16]. A *cell complex* K on Ω is a finite collection of k -cells for $k \in \{0, 1, 2, 3\}$ such that the following conditions hold [17]:

- (i) Distinct k -cells in K have disjoint interiors.
- (ii) The boundary of any k -cell in K is a union of l -cells in K with $l < k$.
- (iii) The union of all cells in K is Ω .
- (iv) The intersection of k -cell and an l -cell in K with $l \leq k$ (if not empty) is a union of cells in K .

Crucially, k -cells as defined above can be *curved*. However, the standard MFD and DGA methods [13] require k -cells to be *planar* (or flat). A k -cell in K is planar if it is contained in a k -dimensional affine plane of \mathbb{R}^3 . For our purposes, 2-cells in K can be either flat or curved; consequently, also 1-cells in K can be either flat, like in a standard polyhedral cell, or curved. For each 3-cell of K we assume the same geometric regularity assumption **(M2)** in [7]. With this assumption on K , we say that K is a *curved grid* on Ω .

We denote the curved grid K as $K = (N, E, F, C)$, where N the set of 0-cells (*nodes*), E the set of 1-cells (*edges*), F the set of 2-cells (*faces*) and C the set of 3-cells (*elements*) in K .

We denote by $|\cdot|$ either the cardinality of a set or the measure of a geometric element in K . For example, $|F|$ is the number of faces in K , $|f|$ is the area of face $f \in F$ and $|c|$ is the volume of element $c \in C$.

Let X be any set among N, E, F, C so that elements of X can be k -cells with $k \in \{0, 1, 2, 3\}$. Given a l -cell y in K , we denote by $X(y)$ the subset defined by

$$X(y) := \{x \in X \mid x \subset \partial y\}, \quad (1)$$

if $k < l$, otherwise,

$$X(y) := \{x \in X \mid y \subset \partial x\}. \quad (2)$$

For example, $F(c) = \{f \in F \mid f \subset \partial c\}$ collects the faces of c and $C(e) = \{c \in C \mid e \subset \partial c\}$ is the cluster of elements containing edge e .

Let us consider a Cartesian system of coordinates with specified origin $\mathbf{0}$ and denote by $\mathbf{x} = (x_1, x_2, x_3)^T \in \mathbb{R}^3$ the coordinates of its generic point. Given a vector $\mathbf{x} = (x_1, x_2, x_3)^T$, we define $\mathbf{x}|_{(i)} := x_i$ for $i \in \{1, 2, 3\}$.

A node $\mathbf{n} \in N$ is a point of \mathbb{R}^3 . A face $f \in F$ is either a curved or a planar 2-cell. For each face $f \in F$, we define its *face vector* \mathbf{f} by

$$\mathbf{f} := \int_f \hat{\mathbf{n}}_f dS, \quad (3)$$

where $\hat{\mathbf{n}}_f$ denotes the unit vector of \mathbb{R}^3 orthogonal to f (at each point) and oriented according to the right-hand rule with respect to the orientation of f .

Remark 1. The integral (3) is the same for every 2-cell spanning the boundary of f as a consequence of the Divergence Theorem.

3. Curved MFD method

In this section we introduce the basic building blocks of the curved MFD method. We focus on a curved grid $K = (N, E, F, C)$, and we give specific definitions only for the vector space \mathcal{F} of face *degrees of freedoms* (DoFs) since similar definitions apply to the vector spaces of DoFs \mathcal{E} and \mathcal{C} corresponding to edges and elements, respectively; see e.g., Section 3 in [12]. Overall, the definitions of the vector space \mathcal{F} and of the discrete divergence \mathbb{D} and curl operator \mathbb{C} are the same of the standard MFD method, while the definition of local reconstruction operators is different and we employ the novel class of P_0 -consistent local reconstruction operators. Nonetheless, the discrete inner products $[\cdot, \cdot]^{\mathcal{F}}$ and the corresponding derived differential operators are constructed from P_0 -consistent local reconstruction operators using the same construction process of the standard MFD method.

3.1. Projection operators

Let \mathbf{J} be a sufficiently regular vector-valued function so that the integrals of its normal components are well defined on each face $f \in F$. The *projection operator* $P^{\mathcal{F}}$ maps \mathbf{J} onto its face DoFs array $\mathbf{J} = P^{\mathcal{F}}(\mathbf{J})$, where the entry $\mathbf{J}|_{(f)}$ of \mathbf{J} corresponding to face f is

$$\mathbf{J}|_{(f)} := \int_f \mathbf{J} \cdot \hat{\mathbf{n}}_f df. \quad (4)$$

The set of all arrays \mathbf{J} defines the vector space $\mathcal{F} = \mathbb{R}^{|F|}$ of face DoFs.

For each cell $c \in C$, let \mathcal{F}_c be $|F(c)|$ -dimensional vector subspace of \mathcal{F} obtained by selecting entries corresponding to each face in $F(c)$. Accordingly, let $P_c^{\mathcal{F}} : W_c^{\mathcal{F}} \rightarrow \mathcal{F}_c$ be the *local projection operator* (on element c), where $W_c^{\mathcal{F}}$ is a suitable finite-dimensional vector space defined in such a way that $P_c^{\mathcal{F}}$ is bijective on \mathcal{F}_c [12, 14]. We denote by $\mathbb{P}_c^{\mathcal{F}}$ the matrix associated with the

restriction of $P_c^{\mathcal{F}}$ to the vector subspace of constant vector fields defined on c . $\mathbb{P}_c^{\mathcal{F}}$ is a matrix of size $|F(c)| \times 3$ and reads

$$\mathbb{P}_c^{\mathcal{F}} = \begin{pmatrix} \vdots \\ \mathbf{f}^T \\ \vdots \end{pmatrix}, \quad (5)$$

where each \mathbf{f} is the face vector of a face $f \in F(c)$. Finally, let $\mathbb{S}_c^{\mathcal{F}}$ be the *restriction matrix* (on element c) of size $|F(c)| \times |F|$ which maps face DoFs in \mathcal{F} to their restriction in \mathcal{F}_c . Each entry $\mathbb{S}_c^{\mathcal{F}}|_{(f,f')}$, corresponding to a face $f \in F(c)$ and a face $f' \in F$, is +1 if $f = f' \in F(c)$ and 0 otherwise.

3.2. Reconstruction operators

Let $R_c^{\mathcal{F}} : \mathcal{F}_c \rightarrow W_c^{\mathcal{F}}$ be the *local reconstruction operator* (on element c) defined as the inverse of map $P_c^{\mathcal{F}}$, which is well-defined thanks to the definition of the finite-dimensional vector subspace $W_c^{\mathcal{F}}$. We define the *average* of local reconstruction operator $R_c^{\mathcal{F}}$ by

$$\overline{R}_c^{\mathcal{F}} := \frac{1}{|c|} \int_c R_c^{\mathcal{F}} dV, \quad (6)$$

and we denote by $\mathbb{R}_c^{\mathcal{F}}$ the associated matrix. In what follows, we will only deal with averages of local reconstruction operators and for convenience we will drop the words ‘‘average’’ and ‘‘local’’ and refer to them simply as reconstruction operators.

Following [12], we require the family $\{\mathbb{R}_c^{\mathcal{F}}\}_{c \in C}$ of reconstruction operators to satisfy the P_0 -consistency property defined as follows (see also Definition 4.1 in [12]).

Definition 3.1 (P_0 -consistent face reconstruction operators). A collection of face reconstruction operators $\{\mathbb{R}_c^{\mathcal{F}}\}_{c \in C}$ is said to be P_0 -consistent if the following two conditions hold:

$$\text{(P1)} \quad \mathbb{R}_c^{\mathcal{F}} \mathbb{P}_c^{\mathcal{F}} = \mathbb{I}_3, \forall c \in C, \quad (7)$$

$$\text{(P2)} \quad \sum_{f \in F(e)} \mathbb{C}|_{(f,e)} \sum_{c \in C(f)} |c| \text{col}_{(f)} \mathbb{R}_c^{\mathcal{F}} = \mathbf{0}, \forall e \in E, e \not\subset \partial\Omega. \quad (8)$$

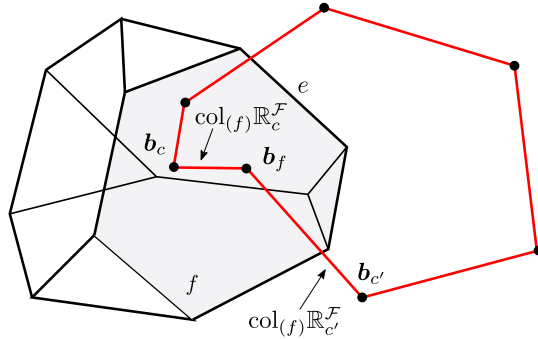


Figure 1: Illustration of property **(P2)** for an internal edge e . In red, the closed path formed by columns (interpreted as vectors of \mathbb{R}^3) of P_0 -consistent reconstruction operators $\{\mathbb{R}_c^{\mathcal{F}}\}_{c \in C(e)}$. Note how this property links reconstruction operators defined on different cells (e.g., the two reconstruction operators $\mathbb{R}_c^{\mathcal{F}}, \mathbb{R}_{c'}^{\mathcal{F}}$ defined on elements $c, c' \in C(e)$ incident on face $f \in F(e)$)

\mathbb{I}_3 denotes the identity matrix of order 3, while \mathbb{C} is the face-edge incidence matrix of K defined in Section 3.4 and $\mathbb{S}_c^{\mathcal{F}}$ is the restriction matrix to element c .

Remark 2. Note that P_0 -consistency is well-defined on a curved grid K . In fact, it involves only the local projection matrices $\{\mathbb{P}_c^{\mathcal{F}}\}_{c \in C}$ whose rows are face vectors of faces of K so that all geometric information of curved faces of K is solely encoded into their face vectors.

The definition of P_0 -consistent reconstruction operators boils down to two requirements. First, property **(P1)** requires that each local reconstruction operator $\mathbb{R}_c^{\mathcal{F}}$ is a left inverse of the local projection operator $\mathbb{P}_c^{\mathcal{F}}$, which is the accuracy property for element-wise constant vector fields. Second, it is easy to check that property **(P2)** has the following geometric interpretation: for each internal edge e of K (i.e., $e \not\subset \partial\Omega$), the vectors $|c| \text{col}_{(f)} \mathbb{R}_c^{\mathcal{F}}$ for each $c \in C(f)$ and each $f \in F(e)$ can be put one after the other to form a geometric closed path, namely, their vector sum is the zero vector; see Fig. 1 for an illustration.

3.3. Discrete inner products

In order to construct the (face) *mass matrix* $\mathbb{M}^{\mathcal{F}}$ associated with the inner product $[\cdot, \cdot]^{\mathcal{F}}$ on \mathcal{F} , we first construct local mass matrices $\{\mathbb{M}_c^{\mathcal{F}}\}_{c \in C}$ for each

element $c \in C$ and then we assemble them using a standard FE assembly process.

For each element $c \in C$, let \mathbb{K}_c be a symmetric and positive-definite matrix of order 3, representing an homogeneous material property in c . We define the local mass matrix $\mathbb{M}_c^{\mathcal{F}}$ (on element c) by

$$\mathbb{M}_c^{\mathcal{F}} := |c|(\mathbb{R}_c^{\mathcal{F}})^T \mathbb{K}_c \mathbb{R}_c^{\mathcal{F}} + \lambda_c (\mathbb{I}_{|F(c)|} - \mathbb{P}_c^{\mathcal{F}} ((\mathbb{P}_c^{\mathcal{F}})^T \mathbb{P}_c^{\mathcal{F}})^{-1} (\mathbb{P}_c^{\mathcal{F}})^T), \quad (9)$$

where $\mathbb{I}_{|F(c)|}$ is the identity matrix of order $|F(c)|$ and λ_c is the scalar factor

$$\lambda_c := \frac{1}{2} \text{trace}(|c|(\mathbb{R}_c^{\mathcal{F}})^T \mathbb{K}_c \mathbb{R}_c^{\mathcal{F}}). \quad (10)$$

In (9), the second term is the so-called *stabilization part* used in the MFD method (e.g. see [1, Lemma 2.9 and Corollary 2.1]), which ensures that matrix $\mathbb{M}_c^{\mathcal{F}}$ is symmetric, positive-definite and remains consistent. We note that other expressions for the stabilization part are possible [18].

The global mass matrix $\mathbb{M}^{\mathcal{F}}$ is constructed by assembling local matrices $\{\mathbb{M}_c^{\mathcal{F}}\}_{c \in C}$ and reads

$$\mathbb{M}^{\mathcal{F}} := \sum_{c \in C} (\mathbb{S}_c^{\mathcal{F}})^T \mathbb{M}_c^{\mathcal{F}} \mathbb{S}_c^{\mathcal{F}}. \quad (11)$$

3.4. Discrete differential operators

Discrete differential operators are represented by incidence matrices of the grid K just like the standard MFD method. Therefore, the *discrete curl operator* is the matrix \mathbb{C} of size $|F| \times |E|$ of incidence numbers between faces and edges. Each entry $\mathbb{C}|_{(f,e)}$, corresponding to a face $f \in F$ and an edge $e \in E$, is: 0, if e is not incident on f (i.e., $e \not\subset f$); +1, if the orientation of e and f are *compatible* [16] according to the right-hand rule, and -1 otherwise. Similarly, the *discrete divergence operator* is the matrix \mathbb{D} of size $|C| \times |F|$ of incidence numbers between elements and faces. Each entry $\mathbb{D}|_{(c,f)}$, corresponding to an element $c \in C$ and a face $f \in F$, is: 0, if f is not incident on c (i.e., $f \not\subset c$); +1, if the orientation of f and c are compatible according to the right-hand rule, and -1 otherwise.

Finally, we can define the *derived discrete gradient operator* $\tilde{\mathbb{G}}$ as the adjoint of the discrete divergence operator \mathbb{D} with respect to the inner product $[\cdot, \cdot]^{\mathcal{F}}$

on \mathcal{F} and the inner product $[\cdot, \cdot]^{\mathcal{C}}$ on \mathcal{C} as

$$[\tilde{\mathbf{G}}\mathbf{U}, \mathbf{J}]^{\mathcal{F}} = [\mathbf{U}, \mathbb{D}\mathbf{J}]^{\mathcal{C}}, \quad \forall \mathbf{U} \in \mathcal{C}, \forall \mathbf{J} \in \mathcal{F}. \quad (12)$$

The inner product $[\cdot, \cdot]^{\mathcal{C}}$ on \mathcal{C} is defined as in [7, Equation (3.12)] (or equivalently, in [1, Equation (2.44)]); note that its definition is actually unique since there is only one quadrature rule for the volume integral on each element that uses a single quadrature point.

4. Properties of P_0 -consistent reconstruction operators

In this section, we derive properties of P_0 -consistent reconstruction operators. In particular, in Section 4.1 we focus on properties that are valid on general curved grids. Here, the central result is Theorem 4, which characterizes P_0 -consistent reconstruction operators as the solution set of the linear system (29). Instead, in Section 4.2, we focus on the practically important case of curved grids obtained by randomly perturbing internal nodes of cubic grids, and in Theorem 7 we establish a special existence result of solutions of linear system (29), and hence, of P_0 -consistent reconstruction operators.

4.1. Structure properties on general curved grids

To start with, we show that P_0 -consistent reconstruction operators $\{\mathbb{R}_c^{\mathcal{F}}\}_{c \in C}$ are defined up to an arbitrary point in \mathbb{R}^3 ; this point can be used to optimize them and we will exploit this possibility in Section 5.

Lemma 1. *For each $c \in C$, let $\mathbf{D}_c := (\dots, \mathbb{D}|_{(c,f)}, \dots)^T$ be the $|F(c)|$ -dimensional vector collecting entries $\mathbb{D}|_{(c,f)}$ for each $f \in F(c)$. Let $\{\mathbb{R}_c^{\mathcal{F}}\}_{c \in C}$ be a family of P_0 -consistent reconstruction operators. Given arbitrary points $\{\mathbf{b}_c\}_{c \in C}$ in \mathbb{R}^3 , we define the family $\{\mathbb{R}_{\mathbf{b}_c}^{\mathcal{F}}\}_{c \in C}$ by*

$$\mathbb{R}_{\mathbf{b}_c}^{\mathcal{F}} := \mathbb{R}_c^{\mathcal{F}} - \frac{1}{|c|} \mathbf{b}_c \mathbf{D}_c^T, \quad \forall c \in C. \quad (13)$$

Then, $\{\mathbb{R}_{\mathbf{b}_c}^{\mathcal{F}}\}_{c \in C}$ is also a family of P_0 -consistent reconstruction operators.

Proof. We need to prove that the family $\{\mathbb{R}_{\mathbf{b}_c}^{\mathcal{F}}\}_{c \in C}$ satisfies properties **(P1)** and **(P2)**.

Proof of **(P1)**. We note that for each element $c \in C$

$$(\mathbb{P}_c^{\mathcal{F}})^T \mathbf{D}_c = \sum_{f \in F(c)} \mathbb{D}|_{(c,f)} \mathbf{f} = \sum_{f \in F(c)} \int_f \mathbb{D}|_{(c,f)} \mathbf{n}_f dS = \int_{\partial c} \mathbf{n}_{\partial c} dS = \mathbf{0}, \quad (14)$$

where the first equality follows from the definition of vector \mathbf{D}_c and matrix $\mathbb{P}_c^{\mathcal{F}}$ while the last one follows from the Divergence Theorem applied to the closed surface ∂c . Therefore, we have that $\mathbb{R}_{\mathbf{b}_c}^{\mathcal{F}} \mathbb{P}_c^{\mathcal{F}} = \mathbb{R}_c^{\mathcal{F}} \mathbb{P}_c^{\mathcal{F}} = \mathbb{I}_3$.

Proof of **(P2)**. We have that

$$\begin{aligned} \sum_{f \in F(e)} \mathbb{C}|_{(f,e)} \sum_{c \in C(f)} |c| \text{col}_{(f)} \mathbb{R}_{\mathbf{b}_c}^{\mathcal{F}} &= \sum_{f \in F(e)} \mathbb{C}|_{(f,e)} \sum_{c \in C(f)} |c| \text{col}_{(f)} \mathbb{R}_c^{\mathcal{F}} - \sum_{f \in F(e)} \mathbb{C}|_{(f,e)} \sum_{c \in C(f)} \mathbb{D}|_{(c,f)} \mathbf{b}_c \\ &= - \sum_{f \in F(e)} \mathbb{C}|_{(f,e)} \sum_{c \in C(f)} \mathbb{D}|_{(c,f)} \mathbf{b}_c, \end{aligned} \quad (15)$$

because the family $\{\mathbb{R}_c^{\mathcal{F}}\}_{c \in C}$ satisfies property **(P2)** by hypothesis. Therefore, we just need to show that the last term in (15) vanishes. We have

$$\begin{aligned} \sum_{f \in F(e)} \mathbb{C}|_{(f,e)} \sum_{c \in C(f)} \mathbb{D}|_{(c,f)} \mathbf{b}_c &= \sum_{c \in C(e)} \sum_{f \in F(c) \cap F(e)} \mathbb{C}|_{(f,e)} \mathbb{D}|_{(c,f)} \mathbf{b}_c \\ &= \sum_{c \in C(e)} (\mathbb{C}|_{(f'_{e,c},e)} \mathbb{D}_{f'_{e,c},c} + \mathbb{C}|_{(f''_{e,c},e)} \mathbb{D}_{f''_{e,c},c}) \mathbf{b}_c = \mathbf{0}, \end{aligned} \quad (16)$$

where $F(c) \cap F(e) = \{f'_{e,c}, f''_{e,c}\}$, and the last equality follows from the identity $\mathbb{D}\mathbf{C} = \mathbf{0}$, due to the cell complex structure of K (see, e.g., [19, Lemma 3.6]). \square

Recall that the boundary $\partial\Omega$ of Ω is *locally flat* if, locally at each of its points, it can be topologically transformed into a plane of \mathbb{R}^3 ; more precisely, if the following is true: for each $\mathbf{x} \in \partial\Omega$, there exist an open neighborhood $U_{\mathbf{x}}$ of \mathbf{x} in \mathbb{R}^3 and a homeomorphism $\phi_{\mathbf{x}} : U_{\mathbf{x}} \rightarrow \mathbb{R}^3$ such that $\phi_{\mathbf{x}}(U_{\mathbf{x}} \cap \partial\Omega) = \{(x_1, x_2, x_3) \in \mathbb{R}^3 : x_3 = 0\}$. Observe that, if $\partial\Omega$ is polyhedral (in the sense of [20, Remark 9.5, p. 93]), then it is also locally flat. By [21], if $\partial\Omega$ is locally flat then $\partial\Omega$ admits a collar in Ω , i.e., there exists an open neighborhood of $\partial\Omega$

in Ω , which is homeomorphic to $\partial\Omega \times [0, 1)$. As an immediate consequence, we have:

Lemma 2. *If $\partial\Omega$ is locally flat, then Ω is simply connected if and only if the interior of Ω in \mathbb{R}^3 is simply connected.*

For other relevant related results, we refer the reader to [22], especially Corollary 3.5 of that paper.

Lemma 3 (Structure of P_0 -consistent reconstruction operators). *Suppose that Ω is simply connected and has a locally flat boundary. Let $K = (V, E, F, C)$ be a curved grid on Ω , and let $\{\mathbb{R}_c^{\mathcal{F}}\}_{c \in C}$ be a family of P_0 -consistent reconstruction operators. Then, there exists a set of points $\{\mathbf{b}_c\}_{c \in C}$ associated with elements of K and a set of points $\{\mathbf{b}_f\}_{f \in F}$ associated with faces of K such that*

$$|c| \operatorname{col}_{(f)} \mathbb{R}_c^{\mathcal{F}} = \mathbb{D}|_{(c,f)}(\mathbf{b}_f - \mathbf{b}_c), \quad \forall c \in C, \forall f \in F(c). \quad (17)$$

Proof. Let $\tilde{G} = (\tilde{V}, \tilde{E})$ be the graph defined as follows: the set of vertices \tilde{V} is $\tilde{V} := C$; the set of edges \tilde{E} contains edge $\{c, c'\}$ if and only if $c \cap c' = f$ for some $f \in F$. We note that graph \tilde{G} is connected since K is.

Let σ be a path in \tilde{G} and denote by $\tilde{E}_\sigma \subset \tilde{E}$ the set of its edges. We fix an orientation on σ by choosing one of the two possible directions to walk on it. Note that all vertices in a path σ are distinct so that each edge $\{c, c'\} \in \tilde{E}_\sigma$ corresponds to a unique face $f \in F$ such that $c \cap c' = f$. Let $\boldsymbol{\sigma} \in \mathbb{R}^{|F|}$ be an array associated to the path σ and defined as follows: $\boldsymbol{\sigma}|_{(f)} \neq 0$ if and only if $f \in \tilde{E}_\sigma$ and, in particular, $\boldsymbol{\sigma}|_{(f)} = +1$ if the orientations of f and σ (as fixed above) are consistent with the right-hand rule, and $\boldsymbol{\sigma}|_{(f)} = -1$ otherwise. We now show that, if σ is closed path, then property **(P2)** implies that

$$\sum_{f \in \tilde{E}_\sigma} \boldsymbol{\sigma}|_{(f)} \sum_{c \in C(f)} |c| \operatorname{col}_{(f)} \mathbb{R}_c^{\mathcal{F}} = \sum_{f \in \tilde{E}_\sigma} \boldsymbol{\sigma}|_{(f)} \sum_{c \in C(f)} \mathbf{r}_{f,c} = \mathbf{0}, \quad (18)$$

where we have defined $\mathbf{r}_{f,c} := |c| \operatorname{col}_{(f)} \mathbb{R}_c^{\mathcal{F}}$ just to simplify notation for the rest of the proof. To prove this fact, let us consider array $\boldsymbol{\chi} \in \mathbb{R}^{|E|}$ such that $\mathbb{C}\boldsymbol{\chi} = \boldsymbol{\sigma}$, which exists thanks to the assumption that Ω is simply connected and has a

locally flat boundary, so Lemma 2 is verified. It follows that

$$\sum_{e \in E, \chi|_{(e)} \neq 0} \chi|_{(e)} \sum_{f \in F(e)} \mathbb{C}|_{(f,e)} \sum_{c \in C(f)} \mathbf{r}_{f,c} = \sum_{f \in \tilde{E}_\sigma} \sigma|_{(f)} \sum_{c \in C(f)} \mathbf{r}_{f,c} = \mathbf{0}, \quad (19)$$

where we have used property **(P2)** and the definition of χ that encodes the fact that “internal” edges in the support of array χ contribute with pairs of opposite sign that mutually eliminates.

We now fix a vertex c^* of \tilde{G} . For any other vertex c of $\tilde{V} \setminus \{c^*\}$ we consider a path σ_c that connects c^* to c in \tilde{G} and we define point \mathbf{b}_{c,σ_c} (with respect to the fixed origin $\mathbf{0}$) by

$$\mathbf{b}_{c,\sigma_c} := \sum_{f' \in \tilde{E}_{\sigma_c}} \sigma_c|_{(f')} \sum_{c' \in C(f')} \mathbf{r}_{f',c'}, \quad (20)$$

where we orient the path by walking on it from c^* to c . Of course, if there exists a unique path σ_c connecting c^* to c we set $\mathbf{b}_c := \mathbf{b}_{c,\sigma_c}$. Otherwise, the crucial aspect of definition (20) is that, thanks to (18), the point \mathbf{b}_{c,σ_c} does not depend on the specific choice of the path σ_c in \tilde{G} as long as it connects c^* to c . As a matter of fact, if we consider a different path σ'_c still connecting c^* to c , then the “union” of these two paths forms the closed path “ $\sigma_c \cup \sigma'_c$ ” for which (18) and (20) yields

$$\mathbf{b}_{c,\sigma_c} = \sum_{f' \in \tilde{E}_{\sigma_c}} \sigma_c|_{(f')} \sum_{c' \in C(f')} \mathbf{r}_{f',c'} = \sum_{f' \in \tilde{E}_{\sigma'_c}} \sigma'_c|_{(f')} \sum_{c' \in C(f')} \mathbf{r}_{f',c'} = \mathbf{b}_{c,\sigma'_c}, \quad (21)$$

where signs are taken into account to represent the fact that σ'_c is walked in opposite sense. Therefore, we set $\mathbf{b}_c := \mathbf{b}_{c,\sigma_c} = \mathbf{b}_{c,\sigma'_c}$.

Next, we define point $\mathbf{b}_{f,c}$ by

$$\mathbf{b}_{f,c} := (\mathbb{D}|_{(c,f)})^{-1} \mathbf{r}_{f,c} + \mathbf{b}_c = \mathbb{D}|_{(c,f)} \mathbf{r}_{f,c} + \mathbf{b}_c \quad (22)$$

for each $c \in C$ and each $f \in F(c)$. Of course, if f is a boundary face, then c is the unique element incident on it and we set $\mathbf{b}_f := \mathbf{b}_{f,c}$. Otherwise, f is the common face of two elements c, c'' , and we now demonstrate that point $\mathbf{b}_{f,c}$ does not depend on the specific element incident on face f . As a matter of fact,

the “union” of paths $\sigma_c, \sigma_{c'}, f$, with f thought as an element of \tilde{E} , forms the closed path “ $\sigma_c \cup \sigma_{c'} \cup \{f\}$ ” for which (18) and (20), (22) yields:

$$\mathbf{b}_c + \mathbb{D}|_{(c,f)}(\mathbf{r}_{f,c} + \mathbf{r}_{f,c'}) - \mathbf{b}_{c'} = \mathbf{0} \quad (23)$$

and hence

$$\mathbf{b}_{f,c} = \mathbf{b}_c + \mathbb{D}|_{(c,f)}\mathbf{r}_{f,c} = \mathbf{b}_{c'} - \mathbb{D}|_{(c,f)}\mathbf{r}_{f,c'} = \mathbf{b}_{c'} + \mathbb{D}|_{(c',f)}\mathbf{r}_{f,c'} = \mathbf{b}_{f,c'}. \quad (24)$$

Therefore, we set $\mathbf{b}_f := \mathbf{b}_{f,c} = \mathbf{b}_{f,c'}$.

To conclude, using (22) and the definition of vectors $\mathbf{r}_{f,c}$ as given above we have that the collection of all points $\{\mathbf{b}_f\}_{f \in F}$ and $\{\mathbf{b}_c\}_{c \in C}$ satisfy

$$|c| \operatorname{col}_{(f)} \mathbb{R}_c^{\mathcal{F}} = \mathbb{D}|_{(c,f)}(\mathbf{b}_f - \mathbf{b}_c), \quad (25)$$

as desired. \square

The two requirements **(P1)** and **(P2)** in Definition 3.1 can be encoded into a linear system of equations by defining suitable matrices $\mathbb{P}^{\mathcal{F}}, \mathbb{R}^{\mathcal{F}}, \mathbb{I}$ (depending on K) as follows.

- Matrix $\mathbb{P}^{\mathcal{F}}$ of size $3|C| \times |F|$. $\mathbb{P}^{\mathcal{F}}$ is the block matrix

$$\mathbb{P}^{\mathcal{F}} = \begin{pmatrix} \vdots \\ (\mathbb{P}_c^{\mathcal{F}})^T (\operatorname{diag} \mathbf{D}_c) \mathbb{S}_c^{\mathcal{F}} \\ \vdots \end{pmatrix}, \quad (26)$$

where $\mathbb{P}_c^{\mathcal{F}}$ is the local projection matrix, $\mathbb{S}_c^{\mathcal{F}}$ the restriction matrix and $\operatorname{diag} \mathbf{D}_c$ is the diagonal matrix of size $|F(c)| \times |F(c)|$ whose main diagonal is the vector \mathbf{D}_c defined in the statement of Lemma 1; see Fig. 2 for a graphical representation of matrix $\mathbb{P}^{\mathcal{F}}$.

- Matrix $\mathbb{R}^{\mathcal{F}}$ of size $|F| \times 3$. $\mathbb{R}^{\mathcal{F}}$ is the block matrix

$$\mathbb{R}^{\mathcal{F}} = \begin{pmatrix} \vdots \\ \mathbf{b}_f^T \\ \vdots \end{pmatrix}, \quad (27)$$

where each point $\mathbf{b}_f \in \mathbb{R}^3$ corresponds to a face $f \in F$.

$$\begin{array}{c}
c'' \\
c \\
c'
\end{array}
\begin{pmatrix}
0 & -\mathbf{f}_j & 0 \\
\vdots & 0 & \mathbf{f}_k \\
\mathbf{f}_i & \vdots & \vdots \\
\cdots & \vdots & \cdots \\
-\mathbf{f}_i & \mathbf{f}_j & \cdots \\
\vdots & \vdots & \vdots \\
0 & 0 & 0
\end{pmatrix}$$

Figure 2: Structure of matrix $\mathbb{P}^{\mathcal{F}}$: face vector of each internal face appears in two different blocks with opposite signs, where the two blocks correspond to the unique two elements sharing the internal face; instead, face vector of each boundary face appears only in one block corresponding to the unique element containing it. For example, the internal face f_i is shared between elements c, c' and its face vector \mathbf{f}_i appears with opposite signs on the rows corresponding to elements c, c' ; the boundary face f_k is contained in the unique element c'' and its face vector \mathbf{f}_k appears only on the rows corresponding to element c'' .

- Matrix \mathbb{I} of size $3|C| \times 3$. \mathbb{I} is the block matrix

$$\mathbb{I} = \begin{pmatrix} \vdots \\ |c|\mathbb{I}_3 \\ \vdots \end{pmatrix}, \quad (28)$$

where $|c|$ denotes the volume of an element $c \in C$ and \mathbb{I}_3 is the identity matrix of order 3.

In what follows, we will also denote matrices $\mathbb{P}^{\mathcal{F}}, \mathbb{R}^{\mathcal{F}}, \mathbb{I}$ as $\mathbb{P}_K^{\mathcal{F}}, \mathbb{R}_K^{\mathcal{F}}, \mathbb{I}_K$ in order to highlight their dependence on geometric elements of the curved grid K .

Remark 3 (Structure of rows of $\mathbb{P}^{\mathcal{F}}$). By definition of block matrix $\mathbb{P}^{\mathcal{F}}$ in (26), a row of $\mathbb{P}^{\mathcal{F}}$ is a row of some block $(\mathbb{P}_c^{\mathcal{F}})^T(\text{diag } \mathbf{D}_c) \mathbb{S}_c^{\mathcal{F}}$ for some element $c \in C$ and thus it collects one among the three coordinates $\mathbf{f}|_{(i)}$ with $i \in \{1, 2, 3\}$ of face vectors decomposing the boundary of c . Therefore, each row of $\mathbb{P}^{\mathcal{F}}$ can be put in one-to-one correspondence with a pair made of an element of C and an index $i \in \{1, 2, 3\}$, and we can identify the set of rows of $\mathbb{P}^{\mathcal{F}}$ corresponding to an index $i \in \{1, 2, 3\}$ with the set of pairs $\Pi_i := C \times \{i\}$. Accordingly, the set of all rows of $\mathbb{P}^{\mathcal{F}}$ is the set $\Pi := \bigcup_{i \in \{1, 2, 3\}} \Pi_i$.

Theorem 4 (Linear system associated with P_0 -consistent reconstruction operators). *Let $K = (V, E, F, C)$ be a curved grid on Ω . Let us consider the linear system of equations*

$$\mathbb{P}_K^{\mathcal{F}} \mathbb{R}_K^{\mathcal{F}} = \mathbb{I}_K, \quad (29)$$

where $\mathbb{P}_K^{\mathcal{F}}$, $\mathbb{R}_K^{\mathcal{F}}$ and \mathbb{I}_K are defined in (26), (27) and (28), respectively. The following two assertions hold.

- (i) *If $\mathbb{R}_K^{\mathcal{F}}$ is a solution of (29), then there exists a family $\{\mathbb{R}_c^{\mathcal{F}}\}_{c \in C}$ of P_0 -consistent reconstruction operators.*
- (ii) *Suppose that Ω is simply connected and has a locally flat boundary, and let $\{\mathbb{R}_c^{\mathcal{F}}\}_{c \in C}$ be a family of P_0 -consistent reconstruction operators. Then, there exists a solution $\mathbb{R}_K^{\mathcal{F}}$ of (29).*

Proof. (i) Let $\mathbb{R}^{\mathcal{F}}$ be a solution of (29). We define the family $\{\mathbb{R}_{\mathbf{0}_c}^{\mathcal{F}}\}_{c \in C}$ by

$$(\mathbb{R}_{\mathbf{0}_c}^{\mathcal{F}})^T := \frac{1}{|c|} (\text{diag } \mathbf{D}_c) \mathbb{S}_c^{\mathcal{F}} \mathbb{R}^{\mathcal{F}}, \quad \forall c \in C. \quad (30)$$

We now show that $\{\mathbb{R}_{\mathbf{0}_c}^{\mathcal{F}}\}_{c \in C}$ is a family of P_0 -consistent reconstruction operators, namely, it satisfies properties **(P1)** and **(P2)**.

Proof of (P1). By definition of block matrix $\mathbb{P}^{\mathcal{F}}$ in (26), we have that equation $(\mathbb{P}_c^{\mathcal{F}})^T (\text{diag } \mathbf{D}_c) \mathbb{S}_c^{\mathcal{F}} \mathbb{R}^{\mathcal{F}} = |c| \mathbb{I}_3$ holds for each element $c \in C$. Transposing members and using the definition of $\mathbb{R}_{\mathbf{0}_c}^{\mathcal{F}}$ we get $\mathbb{R}_{\mathbf{0}_c}^{\mathcal{F}} \mathbb{P}_c^{\mathcal{F}} = \mathbb{I}_3$.

Proof of (P2). We have that

$$\sum_{f \in F(e)} \mathbb{C}|_{(f,e)} \sum_{c \in C(f)} |c| \text{col}_{(f)} \mathbb{R}_{\mathbf{0}_c}^{\mathcal{F}} = \sum_{f \in F(e)} \mathbb{C}|_{(f,e)} \sum_{c \in C(f)} \mathbb{D}|_{(c,f)} \mathbf{b}_f = \mathbf{0} \quad (31)$$

because the second term in (31) vanishes by reasoning as in (16) in the proof of Lemma 1.

(ii) Let $\{\mathbb{R}_c^{\mathcal{F}}\}_{c \in C}$ be a family of P_0 -consistent reconstruction operators and let us apply Lemma 3 to it. Hence, there exist points $\{\mathbf{b}_c\}_{c \in C}$ and $\{\mathbf{b}_f\}_{f \in F}$ such that $|c| \text{col}_{(f)} \mathbb{R}_c^{\mathcal{F}} = \mathbb{D}|_{(c,f)} (\mathbf{b}_f - \mathbf{b}_c)$ for each $c \in C$ and each $f \in F(c)$. Let $\{\mathbb{R}_{\mathbf{0}_c}^{\mathcal{F}}\}_{c \in C}$ be the family of P_0 -consistent reconstruction operators obtained by applying Lemma 1 to $\{\mathbb{R}_c^{\mathcal{F}}\}_{c \in C}$ with points $\{\mathbf{b}_c\}_{c \in C}$ up to a minus sign; it is then

clear that $|c| \operatorname{col}_{(f)} \mathbb{R}_{\mathbf{0}_c}^{\mathcal{F}} = \mathbb{D}|_{(c,f)} \mathbf{b}_f$. Now consider equations $|c| \mathbb{R}_{\mathbf{0}_c}^{\mathcal{F}} \mathbb{P}_c^{\mathcal{F}} = |c| \mathbb{I}_3$ for each element $c \in C$. By transposing members, using the definition of block matrices $\mathbb{P}^{\mathcal{F}}$, \mathbb{I} in (26), (28), and using the points $\{\mathbf{b}_f\}_{f \in F}$ to define $\mathbb{R}^{\mathcal{F}}$ as in (27), we have that the matrix $\mathbb{R}^{\mathcal{F}}$ is a solution of linear system (29). \square

Remark 4 (Dual grid structure associated with P_0 -consistent reconstruction operators). Corresponding to P_0 -consistent reconstruction operators solution of linear system (29) there is a “generalized” dual grid structure as follows. We think each point \mathbf{b}_f in (27) as a “generalized barycenter” of face f (hence, the notation \mathbf{b}_f), and we think each point \mathbf{b}_c as a “generalized barycenter” of element c . Next, we think each pair $(\mathbf{b}_f, \mathbf{b}_c)$, where f is a face of element c , as a “generalized dual edge” with suitable orientation given by the pair order and depending on the coefficient $\mathbb{D}|_{(c,f)}$. See Section 5 for instances of such dual grid structures constructed for the considered test cases.

Let T be a rigid translation of \mathbb{R}^3 and denote by $T(K)$ the curved grid obtained by applying T to each node, edge, face and cell of K . Then, it is easy to see that corresponding linear system $\mathbb{P}_{T(K)}^{\mathcal{F}} \mathbb{R}_{T(K)}^{\mathcal{F}} = \mathbb{I}_{T(K)}$ is equal to (29), as meaning that $\mathbb{P}_{T(K)}^{\mathcal{F}} = \mathbb{P}_K^{\mathcal{F}}$ and $\mathbb{I}_{T(K)} = \mathbb{I}_K$. The next result discusses the case of rigid rotations of K .

Proposition 5 (Transformation of linear system (29) under rigid rotations of K). *Let L be a rigid rotation of \mathbb{R}^3 about the origin $\mathbf{0}$ and let \mathbb{L} the corresponding matrix. Denote by $L(K)$ the curved grid obtained by applying L to each node, edge, face and cell of K . Denote by $\mathbb{P}_{L(K)}^{\mathcal{F}}$, $\mathbb{R}_{L(K)}^{\mathcal{F}}$ and $\mathbb{I}_{L(K)}$ the matrices defined via elements of $L(K)$ as in (26), (27) and (28), respectively. Accordingly, let us consider linear system*

$$\mathbb{P}_{L(K)}^{\mathcal{F}} \mathbb{R}_{L(K)}^{\mathcal{F}} = \mathbb{I}_{L(K)}, \quad (32)$$

and define

$$\mathbb{R}_K^{\mathcal{F}} := \mathbb{R}_{L(K)}^{\mathcal{F}} \mathbb{L}. \quad (33)$$

Then, $\mathbb{R}_K^{\mathcal{F}}$ in (33) is a solution of linear system (29) if and only if $\mathbb{R}_{L(K)}^{\mathcal{F}}$ is a solution of linear system (32).

Proof. Let f be face of K and denote by $f' = L(f)$ be the corresponding rotated face in $L(K)$. Hence, we have that $\mathbf{f}' = \mathbb{L}\mathbf{f}$. Using the block structure of matrix $\mathbb{P}_K^{\mathcal{F}}$ as in (26), we infer that $\mathbb{P}_{L(K)}^{\mathcal{F}} = (\mathbb{I}_{|C|} \otimes \mathbb{L})\mathbb{P}_K^{\mathcal{F}}$, where $\mathbb{I}_{|C|}$ is the identity matrix of order $|C|$. Next, using the block structure of matrix \mathbb{I}_K as in (28), we have that $\mathbb{I}_{L(K)} = \mathbb{I}_K$ since L leave volumes of rotated elements invariant.

Consider now a solution $\mathbb{R}_{L(K)}^{\mathcal{F}}$ of linear system (32). Then, by multiplying (32) by $(\mathbb{I}_{|C|} \otimes \mathbb{L})$ on the left, and by \mathbb{L} on the right, we get

$$\begin{aligned} (\mathbb{I}_{|C|} \otimes \mathbb{L}^T) (\mathbb{P}_{L(K)}^{\mathcal{F}} \mathbb{R}_{L(K)}^{\mathcal{F}}) \mathbb{L} &= (\mathbb{I}_{|C|} \otimes \mathbb{L}^T) (\mathbb{I}_{L(K)}) \mathbb{L} \Rightarrow \\ ((\mathbb{I}_{|C|} \otimes \mathbb{L}^T)(\mathbb{I}_{|C|} \otimes \mathbb{L})) \mathbb{P}_K^{\mathcal{F}} (\mathbb{R}_{L(K)}^{\mathcal{F}} \mathbb{L}) &= \mathbb{I}_{L(K)} \Rightarrow \\ \mathbb{P}_K^{\mathcal{F}} (\mathbb{R}_{L(K)}^{\mathcal{F}} \mathbb{L}) &= \mathbb{I}_K, \end{aligned} \tag{34}$$

where we have used the expressions of rotated matrices $\mathbb{P}_{L(K)}^{\mathcal{F}}, \mathbb{I}_{L(K)}$ together with the block structure of matrix $\mathbb{I}_{|C|} \otimes \mathbb{L}$ and the fact that \mathbb{L} is orthogonal since is the matrix associated with the rigid rotation L of \mathbb{R}^3 . The last relation in (34) shows that $\mathbb{R}_K^{\mathcal{F}}$ in (33) is a solution of (29), and the converse result follows immediately since L^{-1} is again a rotation of \mathbb{R}^3 . \square

4.2. Existence results on cubic grids with randomly perturbed nodes

Let $K = (V, E, F, C)$ be a curved grid on Ω . We now want to determine conditions on the geometry of K for which linear system (29) is compatible. Of course such conditions should restrict the class of curved grids since matrices $\mathbb{P}_K^{\mathcal{F}}, \mathbb{R}_K^{\mathcal{F}}, \mathbb{I}_K$ in (29) depend on the specific geometry of curved grid K . Therefore, we wish to solve the following general problem:

(Pr1) Characterize the set \mathfrak{C} of all curved grids K for which linear system (29) is compatible.

A specific version of **(Pr1)** is the following:

(Pr2) Characterize the subset $\mathfrak{A} \subset \mathfrak{C}$ of all curved grids K such that matrix $\mathbb{P}_K^{\mathcal{F}}$ has full rank, i.e., $\text{rank } \mathbb{P}_K^{\mathcal{F}} = 3|C|$.

Problem **(Pr1)** seems to be very difficult in general and we do not tackle it in the present contribution. Instead, we focus on problem **(Pr2)** and we

determine a sufficient and a necessary condition for the curved grid K to be contained in the class \mathfrak{R} .

4.2.1. A necessary condition

To derive a necessary condition, it is clear that $\text{rank } \mathbb{P}_K^{\mathcal{F}} = 3|C|$ implies $|F| \geq 3|C|$. We now discuss the implications of the condition $|F| \geq 3|C|$ on the geometry of curved grids in \mathfrak{R} . Let us assume that each element $c \in C$ has the same number k of faces. Consider the set Q of all pairs (f, c) for each $c \in C$ and each $f \in F(c)$. Since every element has k faces, we have $|Q| = k|C|$. Moreover, since every internal face is shared by exactly two elements and every boundary face is incident to exactly one element, we have $|Q| = 2|F_{int}| + |F_b|$, where sets F_{int} and F_b partition F into internal and boundary faces, respectively. By combining these equations and plugging into $|F| \geq 3|C|$, we get the equivalent condition $(k-6)|F_{int}| \geq (3-k)|F_b|$, which holds independently of $|F|$ for $k \geq 6$. In order to practically deal with the cases $k = 4$ or $k = 5$ we propose the following construction. For each element $c \in C$ we select a face $f \in F(c)$ to form a sequence of pairs $Q' = (\dots, (f, c), \dots)$ such that each face f does not appear in more than one pair in Q' . Then, if $k = 4$, we partition each face appearing in a pair of the sequence Q' into three polygons, and we deform them to form three linearly independent face vectors. Similarly, if $k = 5$, we partition each face appearing in a pair of the sequence Q' into two polygons, and we deform them to form two linearly independent face vectors. In both cases, in the end we get a curved grid whose elements satisfy the condition $k \geq 6$. Note that a sequence Q' as above can be constructed efficiently in linear time and space using standard spanning tree constructions (e.g. see [23] for a detailed description of such a construction). The price to pay is the additional number of face DoFs which shifts from $|F|$ to $|F| + 2|C|$ for $k = 4$ and $|F| + |C|$ for $k = 5$.

4.2.2. A sufficient condition

To derive a sufficient condition, we restrict to a practically important class of curved grids and for it we prove that the condition $|F| \geq 3|C|$ is sufficient in a very precise sense. Let $K_h = (N_h, E_h, F_h, C_h)$ be a cubic grid whose elements in C_h are cubes of edge length h that are, up to a rigid rotation, subsets of \mathbb{R}^3 of the form $\mathbf{z} + [0, h]^3$ for some $\mathbf{z} \in \mathbb{R}^3$. Following [8], we now define the class $\mathfrak{M}(K_h)$ of curved grids constructed from K_h as follows. Let P_h be the cube $[-0.4h, 0.4h]^3$, let $N_{h,int} \subset N_h$ be the set of internal nodes of K_h , and let $P := \prod_{\mathbf{n} \in N_{h,int}} P_h = (P_h)^{|N_{h,int}|}$. Note that P is a subset of $\mathbb{R}^{3|N_{h,int}|}$ whose interior is the non-empty open set $\prod_{\mathbf{n} \in N_{h,int}} (-0.4h, 0.4h)^3$. For each $\mathbf{n} \in N_{h,int}$, consider a point $\boldsymbol{\xi}_{\mathbf{n}}$ in P_h , and denote by $\Xi = (\dots, \boldsymbol{\xi}_{\mathbf{n}}, \dots)^T$ a $3|N_{h,int}|$ -dimensional array in P . For each array $\Xi \in P$, we define the curved grid $K_{\Xi} = (N_{\Xi}, E_{\Xi}, F_{\Xi}, C_{\Xi})$ associated with Ξ as follows:

- Set of nodes N_{Ξ} . For each node $\mathbf{n} \in N_h$ corresponds the *moved* node $\mathbf{n}_{\Xi} \in N_{h,\Xi}$ defined by

$$\mathbf{n}_{\Xi} := \begin{cases} \mathbf{n} + \boldsymbol{\xi}_{\mathbf{n}} & \text{if } \mathbf{n} \in N_{h,int}, \\ \mathbf{n} & \text{if } \mathbf{n} \in N_{h,b}. \end{cases} \quad (35)$$

In other words, each internal node $\mathbf{n} \in N_{h,int}$ is shifted in a cubic region of edge length $0.8h$ that is centered at point \mathbf{n} and whose edges are aligned with the axes of cubic grid K_h . Instead, each boundary node $\mathbf{n} \in N_{h,b}$ is left invariant.

- Set of edges E_{Ξ} . For each edge $e \in E_h$ with boundary nodes $\{\mathbf{n}_1, \mathbf{n}_2\} = N(e)$ corresponds the edge (segment) e_{Ξ} joining the moved nodes $\mathbf{n}_{1,\Xi}, \mathbf{n}_{2,\Xi}$.
- Set of faces F_{Ξ} . For each face $f \in F_h$ with boundary nodes $\{\mathbf{n}_1, \mathbf{n}_2, \mathbf{n}_3, \mathbf{n}_4\} = N(f)$ and such that ∂f is equal to the following sum of oriented segments $\partial f = [\mathbf{n}_1, \mathbf{n}_2] + [\mathbf{n}_2, \mathbf{n}_3] + [\mathbf{n}_3, \mathbf{n}_4] + [\mathbf{n}_4, \mathbf{n}_1]$ according to a fixed (arbitrary) orientation, corresponds the *piecewise linear* face f_{Ξ} made of two triangles $t_f^{(1)}$ and $t_f^{(2)}$ with vertices $\{\mathbf{n}_{1,\Xi}, \mathbf{n}_{2,\Xi}, \mathbf{n}_{3,\Xi}\}$ and $\{\mathbf{n}_{3,\Xi}, \mathbf{n}_{4,\Xi}, \mathbf{n}_{1,\Xi}\}$, respectively, and oriented so that $\partial t_f^{(1)} = [\mathbf{n}_{1,\Xi}, \mathbf{n}_{2,\Xi}] + [\mathbf{n}_{2,\Xi}, \mathbf{n}_{3,\Xi}] + [\mathbf{n}_{3,\Xi}, \mathbf{n}_{1,\Xi}]$

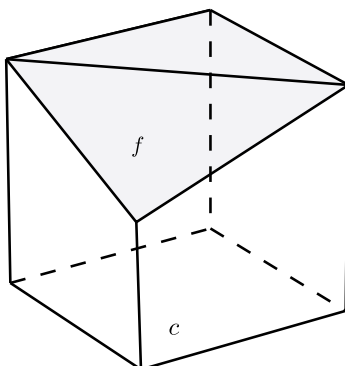


Figure 3: A cube c with a curved face f that is a piecewise linear surface made of two triangles.

and $\partial t_f^{(2)} = [\mathbf{n}_{1,\Xi}, \mathbf{n}_{3,\Xi}] + [\mathbf{n}_{3,\Xi}, \mathbf{n}_{4,\Xi}] + [\mathbf{n}_{4,\Xi}, \mathbf{n}_{1,\Xi}]$. Therefore, thanks to the movement (35), the boundary of each face of f_Ξ is not necessarily a planar quadrilateral; see Fig. 3 for an illustration.

- Set of cells C_Ξ . For each cell $c \in C_h$ corresponds the cell c_Ξ whose boundary is the union of moved faces f_Ξ with $f \in F(c)$.

We define $\mathfrak{M}(K_h)$ as the set of all curved grids K_Ξ for $\Xi \in P$.

The next preliminary result shows that cubic grids K_h belong to the class \mathfrak{R} .

Lemma 6. *Let $K_h = (V_h, E_h, F_h, C_h)$ be a cubic grid. Then, the matrix $\mathbb{P}_{K_h}^{\mathcal{F}}$ has full rank, i.e., $\text{rank } \mathbb{P}_{K_h}^{\mathcal{F}} = 3|C_h|$. In particular, $|F_h| \geq 3|C_h|$.*

Proof. First, observe that the axes of the cubic grid K_h are aligned with the coordinate axes of the chosen Cartesian system of coordinates. For the rest of proof, we denote $\mathbb{P}_{K_h}^{\mathcal{F}}$ by $\mathbb{P}^{\mathcal{F}}$, where we drop subscript K_h just to simplify notation.

Condition $\text{rank } \mathbb{P}^{\mathcal{F}} = 3|C_h|$ holds if and only if there is no linear dependent row vectors of $\mathbb{P}^{\mathcal{F}}$. Let us thus assume that, for the sake of contradiction, that the row vector $\text{row}_{(c,i)} \mathbb{P}^{\mathcal{F}}$, corresponding to element $c \in C$ and i -th coordinate for some $i \in \{1, 2, 3\}$, can be written as linear combination of other rows of $\mathbb{P}^{\mathcal{F}}$,

namely, there exist real coefficients $\{p_{c',j}\}_{(c',j)\in\Pi\setminus\{(c,i)\}}$ such that

$$\text{row}_{(c,i)}\mathbb{P}^{\mathcal{F}} + \sum_{(c',j)\in\Pi\setminus\{(c,i)\}} p_{c',j} \text{row}_{(c',j)}\mathbb{P}^{\mathcal{F}} = \mathbf{0}. \quad (36)$$

Here Π denotes the set of indices defined earlier in Remark 3. Let v be the $|F|$ -dimensional vector that appears in the first member of (36). Without loss of generality, we can assume that $i = 1$ and $h = 1$. Let f_0 be the face of c such that $\mathbf{f}_0 = (1, 0, 0)^T$. Note that f_0 is an internal face of K_h . Otherwise, the column vector $\text{col}_{(f_0)}\mathbb{P}^{\mathcal{F}}$ has exactly one non-zero entry $\mathbb{P}^{\mathcal{F}}|_{(c,f_0)} = 1$ corresponding to element c , and the entry $v|_{(f_0)}$ would be 1 instead of 0 as imposed by (36). Hence f_0 is an internal face of K_h and there exists, and is unique, a cube c_1 of K_h such that $c \cap c_1 = f_0$. Now, the column vector $\text{col}_{(f_0)}\mathbb{P}^{\mathcal{F}}$ has exactly two non-zero entries $\mathbb{P}^{\mathcal{F}}|_{(c,f_0)} = 1$, $\mathbb{P}^{\mathcal{F}}|_{(c_1,f_0)} = -1$ corresponding to c, c_1 . According to (36), it holds that $p_{c_1,1} = 1$. By repeating the above reasoning and using the fact that K_h is bounded, we obtain a sequence $c = c_0, c_1, \dots, c_n$ such that $c_l \cap c_{l+1} = f_l$ with $\mathbf{f}_l|_{(1)} \neq 0$ for $l \in \{0, \dots, n-1\}$, f_l is an internal face of K_h for $l \in \{0, \dots, n-1\}$ and the face f_n of c_n opposite to f_{n-1} is a boundary face of K_h . It follows that the column vector $\text{col}_{(f_n)}\mathbb{P}^{\mathcal{F}}$ has exactly one non-zero entry $\mathbb{P}^{\mathcal{F}}|_{(c_n,f_n)} = 1$. As a consequence, we should have that $v|_{(f_n)} = 1$ and not $v|_{(f_n)} = 0$ as imposed by (36). This gives the desired contradiction. \square

In order to state Theorem 7, we first recall some basic facts about *real algebraic subsets* of \mathbb{R}^m with m an arbitrary natural number [24]. A subset of \mathbb{R}^m is called *real algebraic* if it is the zero set of a family of polynomials with (real coefficients and) variables in \mathbb{R}^m . A basic result is that every real algebraic subset X of \mathbb{R}^m can be written as the union of finite family $\{M_i\}_i$ of smooth submanifolds M_i of \mathbb{R}^m . The dimension $\dim(X)$ of X can be defined as the maximum dimension of the M_i 's. If $\dim(X) < m$ then each M_i has dimension $< m$ and hence each M_i and the whole X have measure zero in \mathbb{R}^m . In particular, the interiors in \mathbb{R}^m of each M_i and of X are empty. It is important to observe that, if X is properly contained in \mathbb{R}^m , i.e., $X \neq \mathbb{R}^m$, then $\dim(X) < m$ so X has measure zero in \mathbb{R}^m . See [24, Chapters 2, 3 and 9] and

[25, Chapter 1, Section 0 and Chapter 3, Section 1].

Theorem 7. *Let $K_h = (N_h, E_h, F_h, C_h)$ be a cubic grid and let $K_\Xi = (N_\Xi, E_\Xi, F_\Xi, C_\Xi)$ be the curved grid in $\mathfrak{M}(K_h)$ obtained by the Ξ -movement (35) of nodes of K_h . Let P' be the set of all $\Xi \in P \subset \mathbb{R}^{3|N_{h,int}|}$ such that the matrix $\mathbb{P}_{K_\Xi}^{\mathcal{F}}$ has not full rank, namely,*

$$P' := \{\Xi \in P : \text{rank}(\mathbb{P}_{K_\Xi}^{\mathcal{F}}) < 3|C_h|\}. \quad (37)$$

Then, P' has measure zero in $\mathbb{R}^{3|N_{h,int}|}$.

Proof. Let $f_\Xi \in F_\Xi$. Rearranging indices if necessary, we can assume that ∂f_Ξ is equal to the following sum of oriented segments $\partial f_\Xi = [\mathbf{n}_{1,\Xi}, \mathbf{n}_{2,\Xi}] + [\mathbf{n}_{2,\Xi}, \mathbf{n}_{3,\Xi}] + [\mathbf{n}_{3,\Xi}, \mathbf{n}_{4,\Xi}] + [\mathbf{n}_{4,\Xi}, \mathbf{n}_{1,\Xi}]$. As a consequence, we have

$$\begin{aligned} \mathbf{f}_\Xi &= \frac{1}{2}(\mathbf{n}_{2,\Xi} - \mathbf{n}_{1,\Xi}) \times (\mathbf{n}_{3,\Xi} - \mathbf{n}_{1,\Xi}) \\ &\quad + \frac{1}{2}(\mathbf{n}_{3,\Xi} - \mathbf{n}_{1,\Xi}) \times (\mathbf{n}_{4,\Xi} - \mathbf{n}_{1,\Xi}), \end{aligned} \quad (38)$$

where “ \times ” indicates the vector product in \mathbb{R}^3 . Using the expression (35) of moved nodes of K_Ξ , we infer that each of the three components of the vector \mathbf{f}_Ξ has a polynomial expression in the variables $(\xi_{\mathbf{n}_{1,1}}, \xi_{\mathbf{n}_{1,2}}, \xi_{\mathbf{n}_{1,3}}, \dots, \xi_{\mathbf{n}_{4,1}}, \xi_{\mathbf{n}_{4,2}}, \xi_{\mathbf{n}_{4,3}})^T = (\boldsymbol{\xi}_{\mathbf{n}_1}, \boldsymbol{\xi}_{\mathbf{n}_2}, \boldsymbol{\xi}_{\mathbf{n}_3}, \boldsymbol{\xi}_{\mathbf{n}_4})^T \in (\mathbb{R}^3)^4$. Note that the latter assertion remains true even if a node $\mathbf{n}_{j,\Xi} = \mathbf{n}_j$ of f_Ξ is a boundary node of K_h and thus is not moved by transformation (35). Indeed, in this case the mentioned polynomial expressions are constant in the variables $(\xi_{\mathbf{n}_j,1}, \xi_{\mathbf{n}_j,2}, \xi_{\mathbf{n}_j,3})^T = \boldsymbol{\xi}_{\mathbf{n}_j}$.

Recall that $3|C_h| \leq |F_h|$ by Lemma 6. Denote by S the family of all subsets of $\{1, \dots, |F_h|\}$ having cardinality $3|C_h|$. For each $F_s \in S$, denote by $\mathbb{P}_{K_\Xi}^{\mathcal{F}}|_{(\Pi \times F_s)}$ the $3|C_h| \times 3|C_h|$ -submatrix of $\mathbb{P}_{K_\Xi}^{\mathcal{F}}$ obtained selecting all the $3|C_h|$ rows and the $3|C_h|$ columns of $\mathbb{P}_{K_\Xi}^{\mathcal{F}}$ whose indices are the elements of the set F_s . Thus, $\{\mathbb{P}_{K_\Xi}^{\mathcal{F}}|_{(\Pi \times F_s)}\}_{F_s \in S}$ is the family of all $3|C_h| \times 3|C_h|$ -submatrices of $\mathbb{P}_{K_\Xi}^{\mathcal{F}}$. Define the function $g : P \rightarrow \mathbb{R}$ by setting

$$g(\Xi) := \sum_{F_s \in S} \left(\det \left(\mathbb{P}_{K_\Xi}^{\mathcal{F}}|_{(\Pi \times F_s)} \right) \right)^2, \quad (39)$$

where “det” is the determinant operation.

Note that g is a polynomial function in the variables $(\dots, \xi_{\mathbf{n},1}, \xi_{\mathbf{n},2}, \xi_{\mathbf{n},3}, \dots)^T = (\dots, \boldsymbol{\xi}_{\mathbf{n}}, \dots)^T = \Xi \in \mathbb{R}^{3|N_{h,int}|}$ since each entry of the matrix $\mathbb{P}_{K_{\Xi}}^{\mathcal{F}}$ is. Observe that $g(\Xi) = 0$ if and only if $\det(\mathbb{P}_{K_{\Xi}}^{\mathcal{F}}|_{(\Pi \times F_s)}) = 0$ for all subsets $F_s \in S$, which is in turn equivalent to assert $\text{rank } \mathbb{P}_{K_{\Xi}}^{\mathcal{F}} < 3|C_h|$. This proves that $P' = P \cap X$, where X is the real algebraic subset of $\mathbb{R}^{3|N_{h,int}|}$ defined by $X := \{\Xi \in \mathbb{R}^{3|N_{h,int}|} : g(\Xi) = 0\}$.

It is important to observe that the polynomial g in (39) is non-zero, i.e., at least one coefficient in the expression of the polynomial g as linear combination of monomials is different from zero. Indeed, by Lemma 6, the rank of $\mathbb{P}_{K_h}^{\mathcal{F}}$ is $3|C_h|$. On the other hand, if $O \in P$ denotes the point associated with the zero vector of $\mathbb{R}^{3|N_{h,int}|}$, then $K_O = K_h$, and it follows that $g(O) \neq 0$, i.e., $O \notin X$. Thus, $X \neq \mathbb{R}^{3|N_{h,int}|}$ and hence X has measure zero in $\mathbb{R}^{3|N_{h,int}|}$. Evidently, the same is true for the subset P' of X . \square

The practical meaning of Theorem 7 is as follows. Let us consider random values for $\Xi = (\dots, \xi_{\mathbf{n},1}, \xi_{\mathbf{n},2}, \xi_{\mathbf{n},3}, \dots)^T \in P$ where each number $\xi_{\mathbf{n},i}$ for $\mathbf{n} \in N_{h,int}$, $i \in \{1, 2, 3\}$ is drawn independently from a uniform distribution on $[-0.4h, 0.4h]$. In this case, it may happen that we hit a point $\Xi \in P'$ so that $\text{rank } \mathbb{P}_{K_{\Xi}}^{\mathcal{F}} < 3|C_h|$. However, thanks to Theorem 7, the probability of this to happen is 0.

We note that the reasoning behind Theorem 7 can be extended to other families of polyhedral grids with randomly perturbed nodes: it is just sufficient to check whether matrix $\mathbb{P}_K^{\mathcal{F}}$ has full rank for a given polyhedral grid K .

4.3. Link between P_0 -consistent and admissible reconstruction operators

The standard MFD method defines the class of *admissible* local reconstruction operators $\{R_c^{\mathcal{F}}\}_{c \in C}$ that satisfy five properties **(R1)**-**(R5)** as defined in [14, 26]. The next result illuminates the link between admissible reconstructions operators and P_0 -consistent reconstruction operators.

Proposition 8. *Let $K = (N, E, F, C)$ be either a polyhedral or a curved grid. For each element $c \in C$, define the dual edge of face $f \in F(c)$ (restricted to c)*

by

$$\tilde{\mathbf{e}}_{f,c} := \mathbb{D}|_{(c,f)}(\mathbf{b}_f^* - \mathbf{b}_c), \quad (40)$$

where \mathbf{b}_f^* is the barycenter of face f and $\mathbf{b}_c \in \mathbb{R}^3$ is an arbitrary point. Let $\{\mathbb{R}_c^{\mathcal{F}}\}_{c \in C}$ be the family of averages of local admissible face reconstruction operators. Then,

$$|c| \operatorname{col}_{(f)} \mathbb{R}_c^{\mathcal{F}} = \tilde{\mathbf{e}}_{f,c}, \quad \forall c \in C, \forall f \in F(c). \quad (41)$$

Moreover, if K is polyhedral, then $\{\mathbb{R}_c^{\mathcal{F}}\}_{c \in C}$ are also P_0 -consistent reconstruction operators.

Proof. Formula (41) is a direct consequence of Equation (35) in Proposition 3.3 of [26], the definition of averages of local reconstruction operators in (6) and the definition (40). The fact that formula (41) defines P_0 -consistent reconstruction operators follows by applying Lemma 3 in [12] and the reasoning to deduce (16) in the proof of Lemma 1. \square

If K is a curved grid then the admissible reconstruction operators in (41) do not satisfy the accuracy property **(P1)**, and a simple example is given by the curved cube in Fig. 3. This inconsistency is the theoretical reason for the lack of convergence of the MFD method on curved grids.

5. Numerical results

In this section we present numerical experiments to test the consistency and convergence of the curved MFD method. We consider a stationary conduction problem as a prototype example of an elliptic boundary value problem. The stationary conduction problem in a domain Ω reads

$$\nabla \times \mathbf{E} = \mathbf{0}, \quad (42a)$$

$$\nabla \cdot \mathbf{J} = 0, \quad (42b)$$

$$\mathbf{J} = \sigma \mathbf{E}, \quad (42c)$$

where \mathbf{E} is the electric field, \mathbf{J} is the current density, and σ is the material parameter electric conductivity.

The boundary $\partial\Omega$ is partitioned as $\partial\Omega = \partial\Omega^c \cup \partial\Omega^{nc}$, where $\partial\Omega^c$ is the subset of $\partial\Omega$ where electrodes are physically placed. We assume that $\partial\Omega^c$ decomposes as the union of $N + 1$ disjoint regions $\{\partial\Omega_i^c\}_{i=0}^N$, each representing a single electrode. For each electrode $\{\partial\Omega_i^c\}_{i=1}^N$ we enforce a corresponding electromotive force $\{U_i\}_{i=1}^N$ with respect to a reference electrode $\partial\Omega_0^c$. On the remaining part of the boundary $\partial\Omega^{nc}$, we impose a homogeneous Neumann boundary condition.

We derive a mixed variational formulation of problem (42) as follows. First, the curl-free condition $\nabla \times \mathbf{E} = \mathbf{0}$ allows us to introduce the scalar potential U such that $\mathbf{E} = -\nabla U$. Next, we introduce the Sobolev space $H(\text{div}, \Omega) = \{\mathbf{v} \in (L^2(\Omega))^3 \mid \nabla \cdot \mathbf{v} \in L^2(\Omega)\}$, and the Sobolev spaces $H_{0, \partial\Omega^{nc}}(\text{div}, \Omega) = \{\mathbf{v} \in H(\text{div}, \Omega) \mid \mathbf{v} \cdot \mathbf{n}_{\partial\Omega} = 0 \text{ on } \partial\Omega^{nc}\}$, $H_0^1(\Omega) = \{q \in L^2(\Omega) \mid \nabla q \in (L^2(\Omega))^3, q = 0 \text{ on } \partial\Omega\}$. The variational formulation reads as: find $\mathbf{J} \in H_{0, \partial\Omega^{nc}}(\text{div}, \Omega)$ and $U \in H_0^1(\Omega)$ such that

$$\int_{\Omega} \sigma^{-1} \mathbf{J} \cdot \mathbf{v} dV - \int_{\Omega} U \cdot \nabla \cdot \mathbf{v} dV = \int_{\Omega} \sigma^{-1} \mathbf{J}_s \cdot \mathbf{v} dV, \forall \mathbf{v} \in H_{0, \partial\Omega^{nc}}(\text{div}, \Omega), \quad (43a)$$

$$\int_{\Omega} \mathbf{J} \cdot \nabla q dV = 0, \forall q \in H_0^1, \quad (43b)$$

where the vector field $\mathbf{J}_s \in H_{0, \partial\Omega^{nc}}(\text{div}, \Omega)$ is introduced to take into account Dirichlet boundary conditions on the electrodes surface $\partial\Omega^c$.

We now introduce the curved MFD discretization of equations (43a), (43b). The train of thought is exactly the same of the standard MFD method except that we employ P_0 -consistent reconstruction operators in place of the standard MFD ones. Therefore, the current density \mathbf{J} is approximated in the vector subspace of face DoFs $\mathcal{F}_{0, \partial\Omega^{nc}} \subset \mathcal{F}$ that collects arrays \mathbf{J} such that $\mathbf{J}|_{(f)} = 0$ for each $f \in \partial\Omega^{nc}$, and the electric potential U is approximated in the vector space of elements DoFs $\mathcal{C} = \mathbb{R}^{|\mathcal{C}|}$. The discrete counterpart of the divergence operator is given by the element-face incidence matrix \mathbb{D} .

In order to define the inner product $[\cdot, \cdot]^{\mathcal{F}}$ on \mathcal{F} , we construct a special family $\{\mathbb{R}_{\mathbf{b}_c}^{\mathcal{F}}\}_{c \in \mathcal{C}}$ of P_0 -consistent reconstruction operators and we proceed in six elementary steps as follows:

1. We compute the points $\{\mathbf{b}_f\}_{f \in F}$, defining rows of matrix $\mathbb{R}^{\mathcal{F}}$ as in (27), as the optimal solution of the following optimization problem:

$$\min_{f \in F} \max_{f \in F} \|\mathbf{b}'_f - \mathbf{b}_f^*\|_{\infty} \quad (44)$$

such that $\{\mathbf{b}'_f\}_{f \in F}$ are a solution of (29),

where points $\{\mathbf{b}_f^*\}_{f \in F}$ are the barycenters of faces and $\|\cdot\|_{\infty}$ is the sup-norm. ²

2. We construct the family $\{\mathbb{R}_{\mathbf{0}_c}^{\mathcal{F}}\}_{c \in C}$ of P_0 -consistent face reconstruction operators using (30) with points $\{\mathbf{b}_f\}_{f \in F}$.
3. We compute the points $\{\mathbf{b}_c\}_{c \in C}$ as

$$\mathbf{b}_c := \frac{1}{|F(c)|} \sum_{f \in F(c)} \mathbf{b}_f, \quad \forall c \in C. \quad (45)$$

4. We construct the family $\{\mathbb{R}_{\mathbf{b}_c}^{\mathcal{F}}\}_{c \in C}$ of P_0 -consistent reconstruction operators using (13) with points $\{\mathbf{b}_c\}_{c \in C}$ and reconstruction operators $\{\mathbb{R}_{\mathbf{0}_c}^{\mathcal{F}}\}_{c \in C}$.
5. We construct the local mass matrices $\{\mathbb{M}_c^{\mathcal{F}}\}_{c \in C}$ using (9) with reconstruction operators $\{\mathbb{R}_{\mathbf{b}_c}^{\mathcal{F}}\}_{c \in C}$.
6. Finally, the mass matrix $\mathbb{M}^{\mathcal{F}}$ is constructed by using (11).

Remark 5. The rationale behind the definitions of points $\{\mathbf{b}_f\}_{f \in F}$ in (44) and $\{\mathbf{b}_c\}_{c \in C}$ in (45) stems from the geometric interpretation of P_0 -consistent reconstruction operators outlined in Remark 4 and ensures that the dual grid structure associated with P_0 -consistent reconstruction operators $\{\mathbb{R}_{\mathbf{b}_c}^{\mathcal{F}}\}_{c \in C}$ is nicely staggered with respect to the given primal grid K ; see Fig. 4 and Fig. 7 for illustrations of such nicely staggered dual grids. In practice, this property is very important because is directly related with optimal properties of local reconstruction operators and thus of local inner products; see [12, Section 5.2].

Remark 6. The particular choice of the sup-norm in the objective function in (44) is motivated by two facts: (i) the unit ball of \mathbb{R}^3 in the sup-norm is a

²The minimization problem (44) can be rewritten as a constrained linear optimization problem using standard manipulations that we omit.

cube; (ii) in the numerical test we will focus only on cubic grids with randomly perturbed nodes.

The mimetic weak formulation of (43a), (43b) reads: find $\mathbf{J} \in \mathcal{F}_{0,\partial\Omega^{nc}}$ and $\mathbf{U} \in \mathcal{C}$ such that

$$[\mathbf{J}, \mathbf{v}]^{\mathcal{F}} - [\mathbf{U}, \mathbb{D} \mathbf{v}]^{\mathcal{C}} = [\mathbf{J}_s, \mathbf{v}]^{\mathcal{F}}, \forall \mathbf{v} \in \mathcal{F}_{0,\partial\Omega^{nc}}, \quad (46a)$$

$$[\mathbb{D} \mathbf{J}, \mathbf{q}]^{\mathcal{C}} = [\mathbf{0}, \mathbf{q}]^{\mathcal{C}}, \forall \mathbf{q} \in \mathcal{C}, \quad (46b)$$

where $\mathbf{J}_s := P^{\mathcal{F}}(\mathbf{J}_s)$ is the projection onto $\mathcal{F}_{0,\partial\Omega^{nc}}$ of the vector field \mathbf{J}_s .

In what follows, we will need the following definitions. Let $K_h = (N_h, E_h, F_h, C_h)$ be a cubic grid with edge length h on a domain Ω , and let $K = (N, E, F, C)$ be a curved grid in $\mathfrak{M}(K_h)$ as defined in Section 4.2.2. Thus, each face $f \in F$ is a piecewise linear surface made of two triangles $t_f^{(1)}, t_f^{(2)}$. We say that a curved face $f \in F$ is *treated as a planar face* if the two triangles $t_f^{(1)}, t_f^{(2)}$ decomposing it are considered as individual faces. For a given $l \in \{0, \dots, |F|\}$, we denote by $K_l = (N_l, E_l, F_l, C_l)$ the curved grid obtained by treating as planar faces a subset of l faces of F . Note that $K = K_0$, and $K_{poly} := K_{|F|}$ is a polyhedral grid with twice the number of faces of K . Finally, by saying that we use the standard MFD or DGA method on the curved grid K_l we mean that we use reconstruction operators (41) in Section 4.3 for each face in F_l , i.e., we use barycenters of faces in F_l to define (40).

5.1. Patch test

We first test the consistency of the curved MFD method by solving a stationary conduction problem whose solution is uniform in a domain Ω .

We consider the cubic domain $\Omega = [0, 1]^3$, and we construct a curved grid $K \in \mathfrak{M}(K_h)$ starting from an initial cubic grid K_h on Ω . We set boundary conditions to generate a uniform current density \mathbf{J} of amplitude 1 and directed downwards along the vertical axis.

Using P_0 -consistent reconstruction operators of the curved MFD method, we exactly reconstruct (up to machine precision) the uniform current

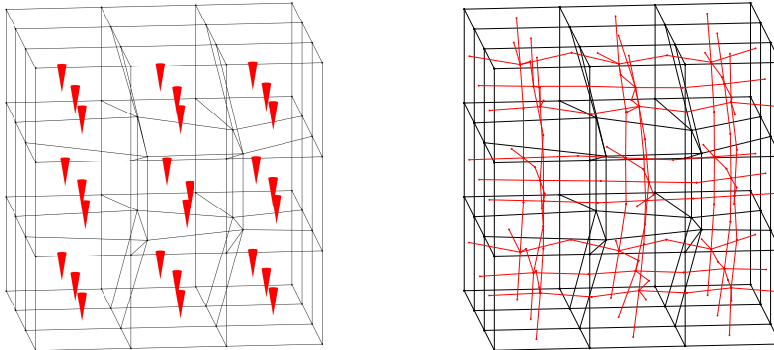


Figure 4: A curved grid partitioning the cubic resistor where all internal faces are curved. On the left, the uniform current density reconstructed inside every curved element; it coincides with the analytical value. On the right, in red, the dual grid structure associated with P_0 -consistent face reconstruction operators solution of (29).

density \mathbf{J} for each curved element of K . In Fig. 4 we picture the resulting reconstructed vector field together with the dual grid associated with the computed P_0 -consistent reconstruction operators on K . Similarly, using the approach in [7] we also reconstruct exactly the uniform current density, but we employ three times more face DoFs.

Using the standard MFD or DGA methods on the curved grid K we potentially employ one DoF for each curved face. However, we do not achieve consistency since the reconstructed field on each element of K is not uniform. To quantitatively measure this consistency error, we compute the relative error on the numerical approximation of the dissipated power of the cubic resistor Ω , and for the considered curved grid K we obtain a 1% relative error.

5.2. Convergence test on randomly perturbed grids

We now test the convergence of the curved MFD method by solving a stationary conduction problem with sufficient smooth solution on a sequence of refined curved grids.

We consider again the cubic domain $\Omega = [0, 1]^3$ and a sequence of refined curved grids $K \in \mathfrak{M}(K_h)$ constructed from a corresponding sequence of cubic grids K_h on Ω with decreasing edge length h .

We measure the convergence of the discrete current density \mathbf{J} solution of (46a), (46b) with the natural norm $\|\cdot\|^\mathcal{F} := [\cdot, \cdot]^\mathcal{F}$ induced by the discrete inner products on the space of face DoFs \mathcal{F} . Specifically, we consider the relative error $e^\mathcal{F}(\mathbf{J})$ defined by

$$e^\mathcal{F}(\mathbf{J}) := \frac{\|\mathbf{J} - \mathbf{J}_e\|^\mathcal{F}}{\|\mathbf{J}_e\|^\mathcal{F}}, \quad (47)$$

where \mathbf{J}_e are DoFs in \mathcal{F} of an exact solution \mathbf{J}_e ; thus the quantity $e^\mathcal{F}(\mathbf{J})$ provides an approximation of the relative error in the L^2 -norm on Ω . In this test, we consider the exact solution $\mathbf{J}_e = -\sigma \nabla U_e$ computed with the harmonic potential

$$U_e(x_1, x_2, x_3) = x_1^2 - 2x_2^2 + x_3^2 \quad \text{in } \Omega. \quad (48)$$

In Fig. 5 we plot the convergence of $e^\mathcal{F}(\mathbf{J})$ for the curved MFD method on the sequence of refined curved grids K . In addition, we also plot the convergence of the standard MFD method applied to the corresponding sequence of polyhedral grids K_{poly} constructed by treating all faces of K as planar. Remarkably, we observe that the curved MFD method achieves the same convergence rate but using half the number of face DoFs.

5.3. Spherical resistor

Next, we test the convergence of the curved MFD method on a computational domain with a curved boundary. In this way, we also test the correctness of boundary conditions on curved boundary faces.

We consider one eighth of a spherical resistor Ω illustrated in Fig. 6. We enforce an electromotive force $U_1 = 1$ V between the external curved electrode $\partial\Omega_1^c$ and the internal one $\partial\Omega_0^c$ so that a current density \mathbf{J} flows along the radial direction.

The domain Ω is partitioned into a curved grid K as schematically illustrated in Fig. 6, where we note that elements of K have also curved edges. In Fig. 8 we plot the convergence of the numerical approximation of the dissipated power versus a sequence of refined grids of the curved MFD method. We also plot the convergence of the standard MFD method applied to the corresponding

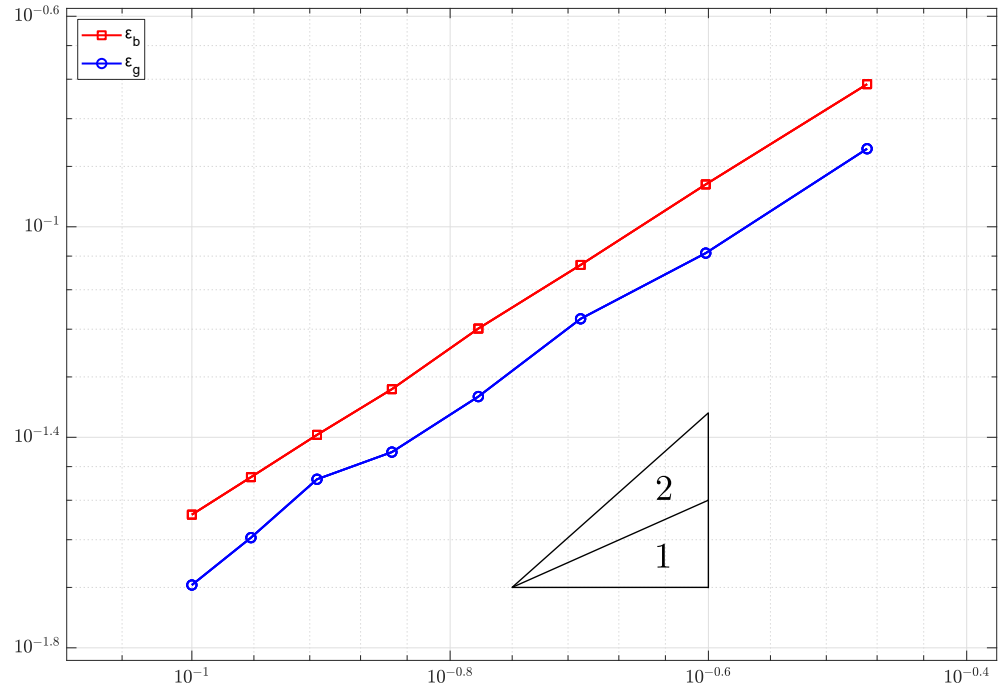


Figure 5: Convergence of the relative error $e^{\mathcal{F}}(\mathbf{J})$ in (47) plotted against the mesh step of the initial unperturbed cubic grids. ϵ_g and ϵ_b represent $e^{\mathcal{F}}(\mathbf{J})$ for the curved MFD method and the standard MFD method where curved faces are approximated by piecewise linear surfaces, respectively. We note that both methods achieve the same convergence rate.

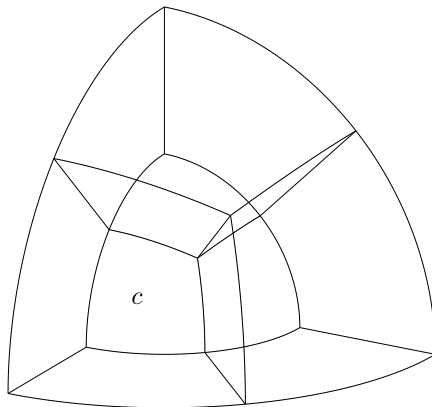


Figure 6: Skeleton of a coarse curved grid partitioning one eighth of a spherical resistor. On the bottom left a curved element c ; we note that every curved element has both curved faces and curved edges.

sequence of polyhedral grids K_{poly} constructed by treating all faces of K as planar; in this case, each curved edge of K is replaced with a straight edge (segment) in K_{poly} .

Interestingly, for coarse grids the curved MFD method gives a better accuracy in the approximation of dissipated power since is not affected by the geometric error made in the approximation of the curved electrodes surface $\partial\Omega^c$ with polygons. For increasing grid sizes, this error tends to zero and the two curves eventually coincide thus giving the same convergence behavior.

5.4. Toroidal resistor

Finally, we compare the curved and the standard MFD method on a same curved grid. As observed in Section 5.1, both schemes employ only one DoF per curved face. However, the standard MFD method on curved grids does not converge, as due to a lack of consistency. Nonetheless, we still want to quantify such consistency error since may be of interest in practical applications.

We consider a toroidal resistor Ω , and we construct a curved grid $K \in \mathfrak{M}(K_h)$ obtained from an initial cubic grid K_h on Ω . We enforce an electromotive force of $U_1 = 1$ V between the external lateral surface $\partial\Omega_1^c$ and the internal one $\partial\Omega_0^c$.

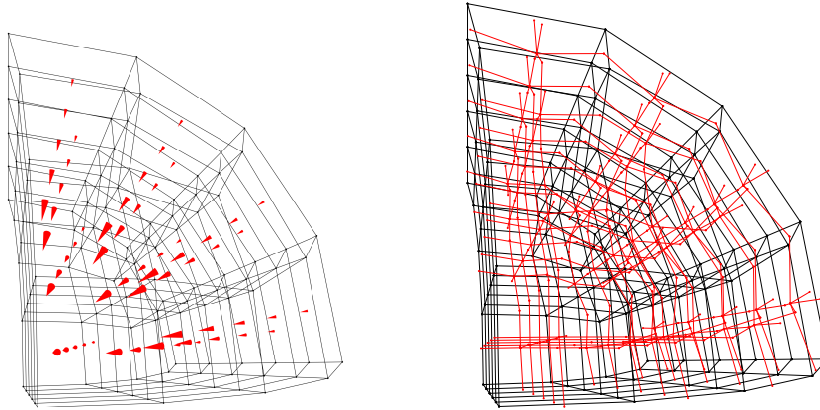


Figure 7: A curved grid partitioning one eighth of a spherical resistor where all internal faces of every element are curved just like in Fig. 6 (the grid nodes are connected by straight edges only for visualization purposes). On the left, the current density reconstructed inside every curved element. On the right, in red, the dual grid structure associated with P_0 -consistent face reconstruction operators solution of (29).

We compute the numerical approximation of the dissipated power of the toroidal resistor for the curved MFD method on K . In Fig. 9, we illustrate the corresponding reconstructed vector field together with the dual grid structure associated with the computed P_0 -consistent reconstruction operators on K . We also compute the same quantity using the standard MFD method on the curved grid K_l .

Then, we compare these two numerical values by computing their absolute difference and dividing it by the analytical value of the dissipated power of the toroidal resistor. The comparison is made by varying the number l of curved faces of K that are treated as planar faces in K_l . By varying l from zero to the number of faces of K , we gradually include more face DoFs. In this way the standard MFD method on K_l gives a discrete problem of increasing size and accuracy. By using the curved grid $K = K_0$, we obtain a 3% relative error. Instead, by using the polyhedral grid K_{poly} (i.e., treating all curved faces of K as planar), we obtain a 0% relative error. This means that, in practice, the numerical value of the dissipated power of the standard MFD method on K_{poly}

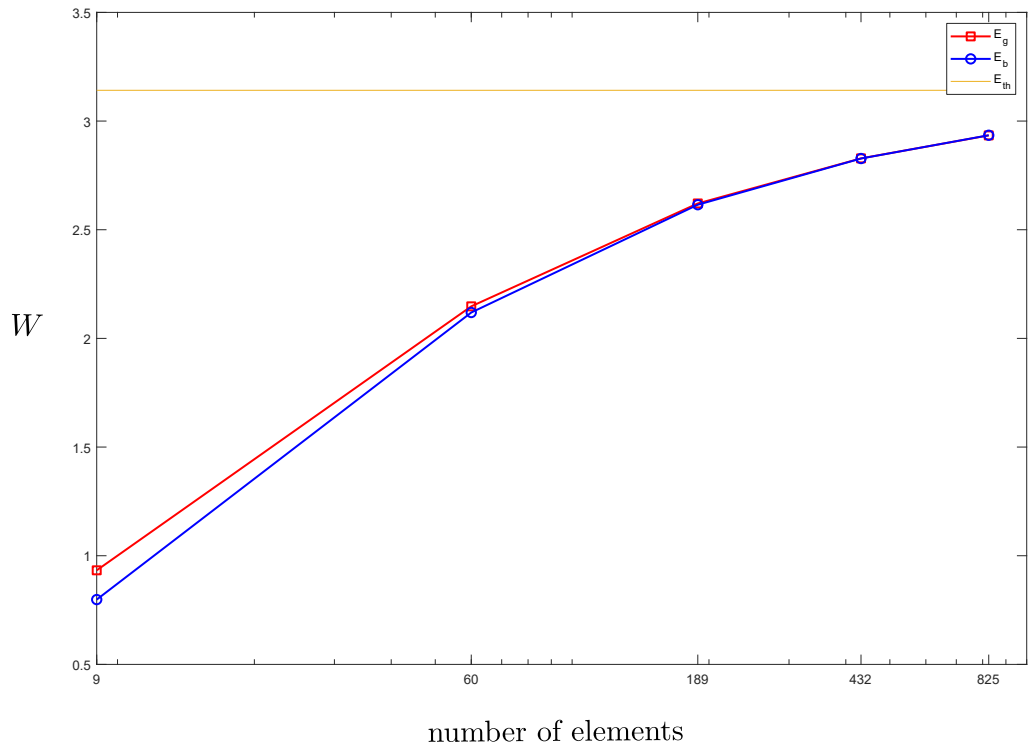


Figure 8: Convergence of the numerical approximation of the dissipated power for grids of increasing size. E_{th} is the reference value equal to πW for the considered one eighth of the spherical resistor domain Ω . E_g and E_b represent the numerical approximation of the dissipated power for the curved MFD method and the standard one, respectively.

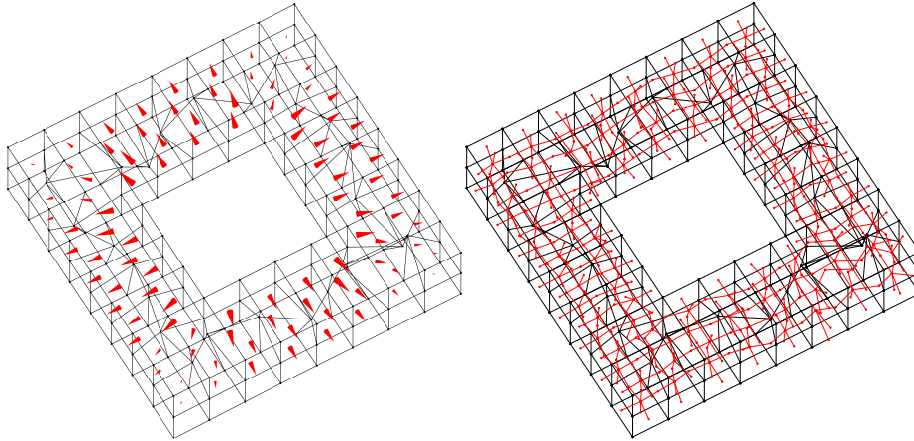


Figure 9: A curved grid partitioning the toroidal resistor where all internal faces of each element are curved. On the left, current density reconstructed inside each curved element. On the right, in red, dual grid structure associated with P_0 -consistent face reconstruction operators solution of (29).

is the same of the curved one on K . However, we note that the number of face DoFs has doubled.

6. Conclusions

In this work, we have proposed a new MFD method that converges on grids with curved faces. The main novelty is that it produces a discrete problem which is symmetric and uses only one DoF per curved face. This has been achieved by employing the new geometrical and topological concept of P_0 -consistent reconstruction operators that generalize the standard MFD reconstruction operators. Indeed, if the grid has no curved faces, the proposed reconstruction operators coincide with the ones of the standard MFD method. The consistency of the new scheme has been tested numerically, demonstrating that the exact solution of the patch test is recovered for discretization grids with curved faces. The convergence results show that the curved MFD method achieves the same accuracy of the standard MFD method where curved faces are partitioned into

planar polygons but without introducing additional DoFs. We also proposed a geometric interpretation of P_0 -consistent reconstruction operators via a dual grid structure. As a result, the concept of dual grid has been generalized to grids with curved faces.

A range of work is slated for future investigation, focusing on further analysis of properties of P_0 -consistent reconstruction operators. In particular, it is our ambition to solve the characterization problem **(Pr1)**. In this paper we have focused on problem **(Pr2)** by proposing a possible solution strategy that, although still needs a deep theoretical analysis, is validated from the practically point of view by Theorem 7 and by the considered numerical experiments. Finally, we expect that the methods introduced in this paper can be extended to high-order methods but their geometric interpretation to be more challenging.

References

- [1] K. Lipnikov, G. Manzini, M. J. Shashkov, Mimetic finite difference method, *J. Comput. Phys.* 257 (2014) 1163–1227.
- [2] K. Lipnikov, M. J. Shashkov, D. Svyatskiy, The mimetic finite difference discretization of diffusion problem on unstructured polyhedral meshes, *J. Comput. Phys.* 211 (2006) 473–491.
- [3] F. Brezzi, K. Lipnikov, V. Simoncini, A family of mimetic finite difference methods on polygonal and polyhedral meshes, *Mathematical Models and Methods in Applied Sciences* 15 (2005) 1533–1551.
- [4] S. Pitassi, F. Trevisan, R. Specogna, Explicit geometric construction of sparse inverse mass matrices for arbitrary tetrahedral grids, *Computer Methods in Applied Mechanics and Engineering* 377 (2021) 113699.
- [5] I. D. Mishev, Nonconforming finite volume methods, *Computational Geosciences* 6 (2002) 253–268.
- [6] I. Aavatsmark, An introduction to multipoint flux approximations for quadrilateral grids, *Computational Geosciences* 6 (2002) 405–432.

- [7] F. Brezzi, K. Lipnikov, M. J. Shashkov, Convergence of mimetic finite difference method for diffusion problems on polyhedral meshes with curved faces, *Mathematical Models and Methods in Applied Sciences* 16 (2006) 275–297.
- [8] F. Brezzi, K. Lipnikov, M. Shashkov, V. Simoncini, A new discretization methodology for diffusion problems on generalized polyhedral meshes, *Computer Methods in Applied Mechanics and Engineering* 196 (2007) 3682–3692.
- [9] L. Yemm, A new approach to handle curved meshes in the hybrid high-order method, *Foundations of Computational Mathematics* (2023) 1–28.
- [10] L. Botti, D. A. D. Pietro, Assessment of hybrid high-order methods on curved meshes and comparison with discontinuous galerkin methods, *J. Comput. Phys.* 370 (2018) 58–84.
- [11] F. Dassi, A. Fumagalli, A. Scotti, G. Vacca, Bend 3d mixed virtual element method for darcy problems, *Computers & Mathematics with Applications* 119 (2022) 1–12.
- [12] S. Pitassi, R. Ghiloni, F. Trevisan, R. Specogna, The role of the dual grid in low-order compatible numerical schemes on general meshes, *J. Comput. Phys.* 436 (2021) 110285.
- [13] L. Codecasa, R. Specogna, F. Trevisan, A new set of basis functions for the discrete geometric approach, *J. Comput. Phys.* 229 (2010) 7401–7410.
- [14] L. B. da Veiga, K. Lipnikov, G. Manzini, *The mimetic finite difference method for elliptic problems*, volume 11, Springer, 2014.
- [15] F. Brezzi, L. D. Marini, Virtual elements on polyhedra with a curved face, *arXiv preprint arXiv:2305.07449* (2023).
- [16] E. Tonti, *The mathematical structure of classical and relativistic physics: A general classification diagram*, 2013.

- [17] S. H. Christiansen, A construction of spaces of compatible differential forms on cellular complexes, *Mathematical Models and Methods in Applied Sciences* 18 (2008) 739–757.
- [18] J. Bonelle, D. A. D. Pietro, A. Ern, Low-order reconstruction operators on polyhedral meshes: application to compatible discrete operator schemes, *Comput. Aided Geom. Des.* 35-36 (2015) 27–41.
- [19] S. H. Christiansen, Foundations of finite element methods for wave equations of maxwell type, in: *Applied wave mathematics*, Springer, 2009, pp. 335–393.
- [20] F. Maggi, *Sets of finite perimeter and geometric variational problems: an introduction to Geometric Measure Theory*, 135, Cambridge University Press, 2012.
- [21] M. Brown, Locally flat imbeddings of topological manifolds, *Annals of Mathematics* (1962) 331–341.
- [22] R. Benedetti, R. Frigerio, R. Ghiloni, The topology of helmholtz domains, *Expositiones Mathematicae* 30 (2012) 319–375.
- [23] S. Pitassi, R. Ghiloni, R. Specogna, Inverting the discrete curl operator: a novel graph algorithm to find a vector potential of a given vector field, *Journal of Computational Physics* 466 (2022) 111404.
- [24] J. Bochnak, M. Coste, M.-F. Roy, *Real algebraic geometry*, volume 36, Springer Science & Business Media, 2013.
- [25] M. W. Hirsch, *Differential topology*, volume 33, Springer Science & Business Media, 2012.
- [26] F. Brezzi, A. Buffa, G. Manzini, Mimetic scalar products of discrete differential forms, *J. Comput. Phys.* 257 (2014) 1228–1259.